W-Pos501

SHRINKAGE-INDUCED INTRACELLULAR ALKALINIZATION IN FIBROBLASTS CAUSED BY HUMAN CYTOMEGALOVIRUS INFECTION.

((A.A. Altamirano, W.E. Crowe and J.M. Russell)) Dept. of Physiology, Medical College of Pennsylvania, Philadelphia, PA 19129.

Infection of human fibroblasts (MRC-5) with human cytomegalovirus (HCMV) produces marked cellular enlargement. The mechanism(s) of development of this cytomegaly are not understood. It is possible that the virus may subvert cell volume regulatory mechanisms such as to result in cell enlargement. Enhanced activity of the Na^+/H^+ exchanger may provide at least some of the additional intracellular solute and obligatory water. This hypothesis was tested by measuring intracellular pH (pH_i), using the fluorescent pH probe BCECF. Seventy-two hours after exposure, the resting pH_i of mock-infected (MI) cells tested in a HEPES-buffered saline solution was 7.38 ± 0.04 (n=10) compared to 7.65 ± 0.03 (n=11) for HCMV-infected (HI) cells. Exposure of MI cells to a 20% hyperosmotic saline solution (57 mM sucrose added) caused a slight acidification ($\Delta pH_i=-0.054 \pm0.006$; n=5), whereas HI cells exposed to the hyperosmotic saline responded with a dramatic alkalinization ($\Delta pH_i=+0.15\pm0.02$;n=4). Five μM diethyl amiloride (DEA) caused an acidification of both HI and MI cells. Upon exposure to 20% hyperosmotic saline, the response of the MI, DEA-treated cells was little changed. However, DEA pretreatment abolished the alkalinization caused by exposure to hyperosmotic saline in HI cells. These results are consistent with HCMV activation of a shrinkage-sensitive acid extrusion mechanism, presumably Na^+/H^+ exchange. Supported by DHHS NS 11946.

STRUCTURE AND FUNCTION OF THE NUCLEAR PORE

Th-AM-SymI-1

CLUES TO NPC ASSEMBLY DERIVED FROM ATYPICAL NINE-FOLD AND 10-FOLD NPCS

J.E. Hinshaw and R.A. Milligan. The Scripps Research Institute, 10666 N. Torrey Pines Rd., La Jolla, CA 92037

Nuclear pore complexes (NPCs) are large supramolecular assemblies located in the nuclear envelope where they provide a channel of communication between the cytoplasm and nucleus. Structural analysis of the NPC to date has focused on NPCs with octagonal rotational symmetry, which have eight radial spokes extending out from the central pore. Occasionally NPCs are found, however, with 9 or 10 spokes. We have examined these unusual NPCs by negative stain electron microscopy and image analysis and compared the results to the data previously obtained from the octagonal NPCs. Comparisons of the two-dimensional projection maps show that the substructure of the spoke is the same in all three forms, 8-fold, 9-fold and 10-fold. Details from the 3 dimensional maps confirms this result, suggesting the spoke is a immutable constituent of the NPC and therefore may be an important building block for NPC assembly. The distance between the annular subunits is equivalent in all three forms which causes the distances between the spokes at higher radius to be smaller in the larger NPCs. For example, the distance between the lumenal subunits is 20Å closer in the 9-fold NPC compared to the 8-fold NPC. This data illustrates that the NPC is flexible to an extent that allows 9 and 10-fold NPCs to form and further suggests that the annular connections are important and may play a role in NPC assembly.

Th-AM-SymI-2

GENETIC ANALYSIS OF NUCLEAR PORE COMPLEX FUNCTION.

((L.I. Davis*◊†, K.D. Belanger†, M.A. Kenna*◊ and S. Wei†)) Howard Hughes Medical Institute*, Department of Genetics◊ and Cell Biology†, Duke University Medical Center, Durham, NC, 27710.

The nuclear pore complex (NPC) is a hetero-oligomeric structure that forms a large channel through the nuclear envelope. It is the only known conduit for export of RNA, and for import of nuclear proteins. A detailed understanding of the mechanism by which the NPC controls macromolecular traffic, and indeed whether it has other functions as well, has been hindered by the complexity of its structure. Among the small number of NPC proteins characterized to date is a family of related polypeptides conserved from vertebrates to yeast. We have used a genetic approach to study the functional and physical relationships between these proteins, and to identify novel proteins involved in NPC function. Temperature sensitive mutants of one of the yeast nucleoporins, *NUP1*, were used to assay the terminal phenotype resulting from loss of function. We found defects in protein import, mRNA export and nuclear envelope structure. To identify novel proteins that are functionally related, we performed a genetic screen for new mutants that are lethal in combination with *nup1* mutations (synthetic lethals). Sixteen mutants were identified, one of which was allelic to *SRP1*. We have now shown that Srp1 is an NPC protein that is physically associated with two of the nucleoporins, Nup1 and Nup2. *srp1* was originally identified by suppression of defective RNA polymerase I. Mutation causes loss of nucleolar integrity and defects in chromosome segregation. The primary structure of *SRP1*, and the phenotypes of *srp1* mutants, suggest that it is required for attachment of the NPC to the underlying nuclear skeleton.

Th-AM-SymI-3

TRANSPORT ACROSS THE NUCLEAR ENVELOPE.

((P.L. Paine, J. Rupesova, and I. Vancurova)) Department of Biological Sciences, St. John's University, Jamaica, NY 11439.

Eukaryotic form makes necessary mechanisms for specific and controlled transport of a variety of materials across the nuclear envelope. Transport of different materials through the nuclear pore complex (NPC) in each direction will be reviewed. Current understanding of mechanisms relies heavily upon the available data pertaining to selective transport of specific proteins from the cytoplasm and their accumulation to higher nuclear vis-a-vis cytoplasmic concentrations. This selective protein transport at the NPC must be viewed as one step of an overall multi-step transport process which also includes important interactions between the transported proteins and other cytoplasmic and intranuclear proteins. Quantitative studies have begun to resolve the transport mechanisms at the level of the NPC from those in the cytoplasm and nucleus and will be examined. Further focus will be on the biophysical nature of the NPC transport machinery and mechanisms, e.g., facilitated diffusion or active transport, as well as coupling of the NPC transport processes to cytoplasmic and intranuclear steps.

Th-AM-SymI-4

ELECTROPHYSIOLOGY OF THE NUCLEAR ENVELOPE.

((Roberta Assandri and Michele Mazzanti)) Dept. Physiology and Biochemistry, I-20133 Milano, Italy

What is the role of ion channels found on the outer nuclear membrane? Channels in the envelope are selective for potassium or chloride. They have conductances from 25 to 1000 pS. The current flowing from the nucleus to the cytoplasm has a time-variant component absent in the other direction. Chemicals interact with and modulate the ionic flux. ATP greatly increases the current and zinc reduces it. Ion channels must underlie the nuclear resting potential recorded in some cells. This could be a transient nucleo-cytoplasmic voltage difference utilized to initiate or to control some nuclear functions. The potential could trigger nuclear envelope breakdown by global constriction. An electrical barrier could regulate nucleo-cytoplasmic traffic. These hypotheses envisage the channel as a bridge across the envelope, but the channels may reside only in the outer membrane. In this case they could be involved in calcium discharge or protein release from the nuclear cisternae. The patch-clamp technique used on either isolated or in *in-situ* nuclei has allowed the observation of 2-3 μ^2 of the outer membrane. Nuclear envelopes from different tissues show a density of pores between 1 and 100 /μ^2. These data suggest that nuclear pores are closed in particular conditions, and that the ion channels may actually be part of the pore complex.

Th-AM-A1

INTRALUMINAL CALCIUM AFFECTS MARKEDLY CALCIUM RELEASE RATES IN TRIADS FROM RABBIT BUT NOT FROM FROG. ((H. Prieto, P. Donoso, P. Rodriguez and C. Hidalgo)) Dept. Physiol. Biophys., Fac. Med., U of Chile and C.E.C.S., Santiago, Chile. (Spons. by M. T. Núñez).

Triads isolated from rabbit or frog skeletal muscle were passively equilibrated with 0.05-10 mM $^{45}CaCl_2$. The amount of calcium accumulated increased as the sum of a saturable (max: 120 and 158 pmol/mg, $K_{0.5}$: 1.2 and 1.1 mM, in rabbit and frog, respectively) plus a linear component. Release was induced by mixing with 2 mM ATP, pCa 5, pH 6.8 in a rapid filtration device (Biologic). In triads from rabbit, release rate constants (k) increased from virtual zero at 0.05-0.1 mM calcium, to 8 s^{-1} in the range 1-10 mM calcium, with a peak around 0.5 mM, suggesting a correlation between calsequestrin calcium binding and release (Ikemoto et al., Biochemistry 28:6764,1989). In contrast, k values were 3 s^{-1} at 0.05-1 mM calcium, and increased to 10-12 s^{-1} at 1.5-10 mM in frog, suggesting that a fraction of calcium release is independent of calsequestrin. Stopped-flow tryptophan fluorescence measurements indicate that in calsequestrin purified from rabbit the rates of calcium association and dissociation are faster than 1 ms at 22 °C, suggesting that the putative control of release by calsequestrin is not due to calcium dissociation from this protein. (Supported by Fondecyt 1108/91, 193/1053 and by the Guggenheim Foundation).

Th-AM-A2

DEPOLARIZATION-INDUCED CALCIUM RELEASE IN TRIADS ISOLATED FROM FROG SKELETAL MUSCLE. ((C. Hidalgo[1], B. Antoniu[2] and N. Ikemoto[2])). [1]Dept. Physiol. Biophys., Fac. Med., University of Chile and Centro de Estudios Científicos de Santiago, Santiago, Chile; [2]Boston Biomedical Research Institute and Dept. Neurol. Harvard Med. Sch., Boston, MA, USA.

Transverse tubules, forming part of triads isolated from frog skeletal muscle, were polarized (cytoplasmic side negative) by the action of the tubular sodium pump. In 150 mM K-gluconate, 15 mM Na-gluconate, the vesicles reached steady state polarization 2 minutes after ATP addition, as measured by the distribution of the charged molecule [^{14}C]-SCN (Ikemoto et al., BBRC 184:538,1992). Addition of 15 mM NaCl decreased markedly the potential difference generated, consistent with a significant tubular chloride permeability. In parallel the sarcoplasmic reticulum moiety was actively loaded with calcium. The polarized triads were depolarized by mixing in a stopped-flow device with a solution containing 150 mM Na gluconate, 15 mM K gluconate, and calcium release was measured using fluo-3 as Ca^{2+} probe. Depolarization caused fast calcium release, with a rate constant of 16 s^{-1}. No release took place in the absence of depolarization. These results suggest that triads isolated from frog skeletal muscle retain the ability to release calcium in response to transverse tubule depolarization, and extend previous results (Ikemoto et al., JBC 259:13151, 1984) obtained with triads isolated from rabbit skeletal muscle to frog muscle, which is commonly used for physiological E-C coupling studies. Supported by FONDECYT 1108/91, Guggenheim Foundation and NIH AR16922.

Th-AM-A3

CALCIUM RELEASE COMPARED IN MAMMALIAN AND AMPHIBIAN SKELETAL MUSCLE FIBERS. ((N. Shirokova, J.García*, G.Pizarro+ and E. Rios)) Rush Univ., Chicago, IL 60612; *Colorado State Univ., Fort Collins, CO 80523; +Univ. de la Republica, Montevideo, Uruguay.

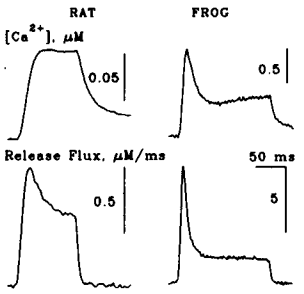

During voltage-clamp depolarization of skeletal muscle fibers, the flux of calcium release has two components: one rapidly inactivating ("peak") and one steady. It has been proposed (Rios and Pizarro, 1989) that these components correspond respectively to "unpaired" release channels and to those "paired" or covered by voltage sensor tetrads of the T tubule (Block et al., 1989). The proportion of ryanodine receptors (release channels) to dihydropyridine receptors (voltage sensors) is two-fold greater in amphibian than in mammalian muscle (Cohn et al., Biophys.J., 64,1993). We tested the consequent prediction, that the ratio peak/steady release flux should be greater in amphibians. We determined release flux in rat EDL and frog semitendinous fibers, in solutions and conditions as similar as possible, using APIII and Fluo-3 as Ca indicators. The figure shows representative Ca transients and release fluxes, elicited by a pulse to -40 mV, in fibers containing high intracellular [EGTA]. In 4 rat fibers at slack length and 5 fibers stretched to 3.8 μm per sarcomere, the ratio was essentially independent of voltage beyond -50 mV and ranged from 2 to 4 (16°C). The average value for frog in similar conditions was 8. The results are consistent with the hypothesis that unpaired release channels contribute the peak component of the release flux. Supported by NIH.

Th-AM-A4

SIMON'S PARADOX. LOCAL INACTIVATION OF Ca RELEASE IN SKELETAL MUSCLE. ((G.Pizarro* and E. Rios)) Dept. Physiology, Rush University, Chicago, IL 60612 and *Depto. de Biofisica, Medicina, U. de la Republica, Montevideo, Uruguay.

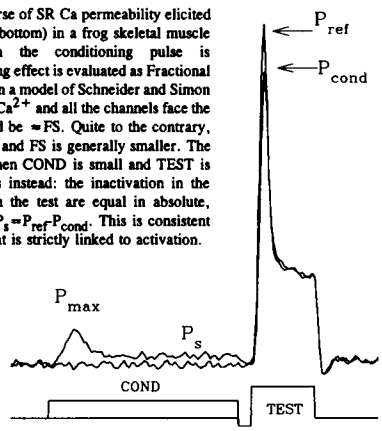

Top figure shows time course of SR Ca permeability elicited by a double voltage pulse protocol (bottom) in a frog skeletal muscle fiber. Fractional Inactivation in the conditioning pulse is $FI=(P_{max}-P_s)/P_{max}$. The conditioning effect is evaluated as Fractional Suppression $FS=(P_{ref}-P_{cond})/P_{ref}$. In a model of Schneider and Simon (1988) this inactivation is caused by Ca^{2+} and all the channels face the same $[Ca^{2+}]$. In this view FI should be =FS. Quite to the contrary, FI is large at essentially all voltages and FS is generally smaller. The discrepancy is especially marked when COND is small and TEST is large. A much simpler rule applies instead: the inactivation in the conditioning and the suppression in the test are equal in absolute, rather than fractional values: $P_{max}-P_s=P_{ref}-P_{cond}$. This is consistent with a mechanism of inactivation that is strictly linked to activation. Only the channels that open seem to inactivate. This would be consistent with a Ca-dependent mechanism if it occurred locally, at the high $[Ca^{2+}]$ prevailing near open channels.
Supported by NIH and AHA.

Th-AM-A5

SUPPRESSION OF Ca RELEASE IN SKELETAL MUSCLE FIBERS BY HIGH AFFINITY Ca INDICATORS IS VOLTAGE DEPENDENT. ((E. Rios, N. Shirokova and G. Pizarro*)) Dept. of Physiology, Rush University, Chicago IL 60612, and *Depto. de Biofisica, Medicina, U. de la Republica, Montevideo, Uruguay.

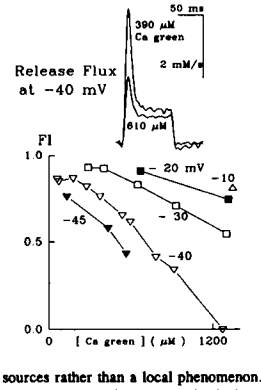

The flux of Ca release from the SR was determined in frog skeletal muscle fibers in a vaseline gap from signals of Ca green and Fluo-3. Ca release was monitored at different voltages as [dye] increased by diffusion from the cut fiber ends. [dye] was sufficiently high to take up most of the released Ca^{2+}. This resulted in quite accurate determinations of release flux. As [dye] increased, the peak of release R_{max} became smaller and the steady level R_s remained constant or decreased. The Fractional Inactivation $(FI=(R_{max}-R_s)/R_{max})$ decreased at all voltages, but its decrease required higher [dye] at higher voltage. The effect was probably due to the buffer properties of the dye as it correlated well with the product $[dye]\times k_{on\ Ca:Dye}$ for different dyes or dye/BAPTA combinations. The results suggest that a) the peak component of release is induced by an increase in $[Ca^{2+}]_i$ (Jacquemond et al. 1991) and b) this increase in "trigger Ca" is a collective function of multiple voltage-controlled Ca sources rather than a local phenomenon. Activation by Ca seems to be global while inactivation is local (preceding communication).

We thank Mike Kuhn (Molec. Probes). Supported by NIH and AHA.

Th-AM-A6

INTRASARCOMERIC CALCIUM GRADIENTS IN SINGLE SKELETAL MUSCLE FIBERS. ((Ariel Escobar, Jonathan Monck*, Julio Fernandez* and Julio Vergara)). Department of Physiology, UCLA, Los Angeles, CA 90024 and *Department of Physiology and Biophysics, Mayo Clinic, Rochester, MN 55905.

For nearly 25 years it has been hypothesized that the change in $[Ca^{2+}]$ in skeletal muscle fibers is generated by the release of Ca^{2+} ions from the terminal cisternae (TC) of the sarcoplasmic reticulum (SR), in response to the depolarization of the transverse tubules (t-tubules). Nevertheless, to date, there is no functional evidence on the exact location at which Ca^{2+}-release takes place. We have used two independent novel methodologies, confocal spot detection of Ca^{2+}-transients and pulsed-laser Ca^{2+}-imaging, to investigate the temporal and spacial distribution of the increment in $[Ca^{2+}]$. Confocal Ca^{2+}-transients (rhod2 and calcium green-5N) recorded at the center of the sarcomere (M-lines) reported slower rising phases, but without an additional lag, than those recorded close to the t-tubules. In addition, "snapshot" (300 ns) fluorescence images (rhod2) revealed prominent high fluorescence bands along the Z-lines when acquired during the early phase of the Ca^{2+} transient, but few inhomogeneities when acquired 15 ms (or later) after the action potential. Both techniques converge in establishing that the release of Ca^{2+} ions is initiated close to the t-tubules. Nevertheless, the kinetics of the localized transients and the patterns of $[Ca^{2+}]$ distribution observed suggest that the release process may not occur exclusively at the highly localized region of the junctional TC but also at other regions of the SR. (Supported by USPHS AR-25201 and MDA)

Th-AM-A7

TWO EFFECTS OF A VOLTAGE PREPULSE ON SARCOPLASMIC RETICULUM (SR) CALCIUM RELEASE IN FROG CUT MUSCLE FIBERS. ((D.-S. Jong, P.C. Pape, *S.M. Baylor, & W.K. Chandler)) Dept. of Cell. & Mole. Physiology, Yale Univ. School of Medicine, New Haven, CT 06510 & *Dept. of Physiology, Univ. of Pennsylvania, Philadelphia, PA 19104

SR Ca release was measured with the EGTA(20 mM)-phenol red method in voltage-clamped fibers mounted in a double Vaseline-gap chamber (Chandler et al., 1992, *Biophysical Journal*, **61**, A130; sarcomere length, 3.4 μm; temperature, 14°C). The pulse protocol was a 10-15 ms prepulse to -20 mV, a 10-150 ms repolarization to -90 mV, and finally a test pulse to -20 mV. In a typical experiment, the peak amplitude of the depletion-corrected rate of Ca release for a test pulse divided by that for a prepulse was 0.65 with a repolarization interval of 10 ms and 0.98 with 150 ms; the time course of recovery was exponential with a time constant of 56 ms. This reduction in amplitude and the time course of its recovery are consistent with the properties of Ca inactivation of Ca release observed in fibers in which the free [Ca] transient was not suppressed by EGTA (Schneider and Simon, 1988, *Journal of Physiology*, **405**, 727). The prepulse also delayed the onset of SR Ca release during the test pulse, although there was little or no change in intramembranous charge movement. In the same experiment, the time to half-peak was delayed 2.9 and 0.6 ms with a 10 and 150 ms repolarization, respectively; this delay followed a decreasing exponential function, with a time constant of 22 ms, plus a constant, 0.6 ms. It is not known whether this delay is related to Ca inactivation of Ca release or to some other process that may or may not be caused by Ca. *Supported by NIH AR-37643.*

Th-AM-A8

A COMPONENT OF CHARGE MOVEMENT TEMPORALLY COUPLED TO THE CALCIUM RELEASE SIGNAL. ((Chiu Shuen Hui)) Dept. of Physiol. and Biophys., Indiana Univ. Med. Ctr., Indianapolis, IN 46202, USA.

Charge movement and calcium transient were measured simultaneously in stretched cut frog twitch fibers (sarcomere length ~4 μm) with the double Vaseline-gap voltage clamp technique. The end-pool solution contained (in mM): 42.5 Cs.glutamate, 20 Cs_2.EGTA, 5.5 Mg.ATP, 20 Cs_2.creatine phosphate, 5 glucose, 20 Cs.MOPS, 1.8 total Ca, 0.6-0.7 antipyrylazo III. The center-pool solution contained (in mM): 108 TEA.CH_3SO_3, 5 Rb_2SO_4, 2 $Ca(CH_3SO_3)_2$, 5 TEA.MOPS, 10^{-3} tetrodotoxin. In addition to the usual I_β and I_γ components, another component was observed in the ON-segments of charge movement traces recorded in the appropriate potential range. This new component followed the I_γ hump and had a time course closely coupled with that of the inactivatable component of the calcium release signal estimated from the Ca-indicator signal. The new charge movement component will be referred to as I_δ. Based on the temporal correlation between I_δ and the calcium release signal and on the fact that I_δ was not observed when the end-pool solution contained 20 mM EGTA without added Ca, it is hypothesized that I_δ might be caused by Ca^{2+} released from the sarcoplasmic reticulum, i.e. it may be the "feedback component". Furthermore, since I_γ precedes I_δ and the calcium release signal, I_γ cannot be caused by calcium release but can be the trigger for calcium release, i.e. it may be the "trigger component". (Supported by NIH NS-21955 and a grant from MDA).

Th-AM-A9

MEASUREMENT OF RESTING $[Ca^{2+}]_i$ IN FROG SKELETAL MUSCLE FIBERS WITH FURA-2 CONJUGATED TO DEXTRAN. ((M. Konishi and M. Watanabe)) Departent of Physiology, Jikei University School of Medicine, Tokyo 105, JAPAN.

To estimate resting cytoplasmic $[Ca^{2+}]$ ($[Ca^{2+}]_i$), single frog skeletal muscle fibers were injected with fura-2 conjugated to dextran (fura dextran, MW 10,000; Molecular Probes, Inc.; K_D for Ca^{2+}, 0.52 μM). After the indicator fluorescence was measured from the resting fibers at 17°C, 5 μM β-escin was applied to permeabilize the cell membrane to relatively small molecules. The slow decline of fura-dextran fluorescence in the β-escin treated fibers suggested the slow leak of the 10 kD molecules out of the fibers. The small molecules (e.g. Ca^{2+}), on the other hand, appeared to quickly diffuse across the cell membrane; changes in bathing solution $[Ca^{2+}]$ to various levels (pCa 7 - 4) caused the change in the Ca^{2+}-dependent fluorescence of fura dextran, which reached the new steady level within a few minutes. The average values for the fraction of Ca^{2+}-bound indicator and K_D for Ca^{2+}, thus estimated for fura dextran in the cytoplasm, were 0.061 and 0.84 μM, respectively. With these values estimated *in vivo*, average resting $[Ca^{2+}]_i$ was calculated to be 55 nM. The results suggest that the high molecular weight Ca^{2+} indicators can be used in combination with the permeabilization technique.

Th-AM-A10

SKELETAL MUSCLE EXCITATION-CONTRACTION COUPLING: GTP$_\gamma$S STIMULATION OF Ca^{2+}-INDUCED Ca^{2+} RELEASE. ((S.K. Donaldson, L.V. Thompson and D.A. Huetteman)) University of Minnesota, Minneapolis, MN 55455.

Peeled (sarcolemma mechanically removed) single fibers from rabbit adductor magnus are capable of transverse tubule (TT) depolarization-induced sarcoplasmic reticulum (SR) Ca^{2+} release via the physiologic excitation-contraction (EC) coupling mechanism (Donaldson, *JGP*, 86:501-525, 1985). Sealed TT within the peeled fiber preparation are polarized and depolarized by ionic diffusion potentials established by variations in the ionic composition (K^+, choline, propionate, Cl^- at constant $[K^+][Cl^-]$) of the peeled fiber bathing solutions. SR Ca^{2+} release is detected as a Ca^{2+}-activated isometric tension transient. The magnitude of the peak of this tension transient is normalized to the maximum Ca^{2+}-activated tension generation for each fiber. When GTP$_\gamma$S (50-75μM) is applied concurrently with TT depolarization, the SR Ca^{2+} release is augmented relative to control in the absence of GTP$_\gamma$S (paired data). GTP$_\gamma$S causes this augmentation by stimulating a G protein (Carney-Anderson & Donaldson, *Biophys J*, 64:A36, 1993). The GTP$_\gamma$S augmentation of SR Ca^{2+} release is selectively eliminated by treatment of the peeled fiber with 5mM procaine added to the bathing solutions. Since 5mM procaine also inhibits the SR Ca^{2+} release stimulated by 10mM bath caffeine in the same fibers, the GTP$_\gamma$S augmentation appears to occur through the Ca^{2+}-induced Ca^{2+} release mechanism. Supported by NIH AR 35132.

MOLECULAR RECOGNITION

Th-AM-B1

DIFFERENTIAL MOBILITY OF REGIONS WITHIN THE TRANSFORMING GROWTH FACTOR-α UPON BINDING TO THE EPIDERMAL GROWTH FACTOR RECEPTOR. ((D.W. Hoyt [a], R.N. Harkins [b], M. Debanne [c], M. O'Connor-McCourt [c], and B.D. Sykes [a])) [a]Protein Engineering Network of Centres of Excellence, University of Alberta, Edmonton, AB, T6G 2S2, Canada; [b]Berlex Biosciences, Richmond, CA, 94804, USA; and [c]Biotechnology Research Institute, Montreal, PQ, H4P 2R2, Canada (Spon. by R.S. Hodges [a])

The interaction of transforming growth factor α (TGF-α) with the complete extracellular domain of the epidermal growth factor receptor (EGFR-ED) was examined by NMR spectroscopy. The ^1H NMR resonances of the methyl groups of TGF-α were used as probes of the mobility of TGF-α when bound to the receptor. Effects on the ^1H NMR relaxation rates ($1/T_1$ and $1/T_2$) of TGF-α methyl resonances caused by binding to 85 kDal EGFR-ED were studied. The relaxation rate enhancements vary for different regions within the bound TGF-α molecule. Resonances from the flexible C-terminus of free TGF-α were broadened significantly upon binding to the EGFR-ED along with resonances in the less flexible interior. However, methyl resonances from the flexible N-terminus remained sharp, indicating a retention of mobility of this region upon binding to the EGFR-ED. These data are discussed in light of a working model for TGF-α binding to EGFR.

Th-AM-B2

ADHESIVE FORCES BETWEEN LIGAND AND RECEPTOR MEASURED BY AFM. ((V.T. Moy, E.-L. Florin and H.E. Gaub)) Physikdepartment, Technische Universität München, 85748 Garching, Germany (Spon. by E. Sackmann)

Since its conception, the AFM has been used to image a wide range of samples, including soft, easily perturbed biological materials. Although a number of imaging modes have been developed in recent years, the images obtained by these techniques are primarily derived from the hard-core repulsion between AFM tip and sample. An imaging mode based on the specific recognition of defined functional group on the sample by receptor molecules on the AFM tip may prove to be beneficial, especially in complex specimens such as the cell membrane. A pre-requisite toward this goal is the development of AFM tips functionalized with ligand specific receptors. Here, we report the fabrication of tips functionalized with avidin and with antibodies. These functionalized tips were characterized by force scan measurements on immobilized ligands on elastic polymer beads. The specificity of the interaction between tip and sample was demonstrated by specific blocking of the ligands or the receptors. The overall adhesive force was analyzed in different models.

Th-AM-B3

THREE-DIMENSIONAL STRUCTURE OF A SINGLE FILAMENT IN THE *LIMULUS* ACROSOMAL BUNDLE: SCRUIN BINDS TO HOMOLOGOUS MOTIFS IN ACTIN. ((M. F. Schmid, J. M. Agris, J. Jakana, P. Matsudaira* and W. Chiu)) Verna and Marrs McLean Department of Biochemistry and The W.M. Keck Center for Computational Biology, Baylor College of Medicine, Houston, TX 77030 *Whitehead Institute for Biomedical Research and Department of Biology, Massachusetts Institute of Technology, Cambridge, MA 02142

Frozen, hydrated acrosomal bundles from *Limulus* sperm were imaged with a 400 kV electron cryomicroscope. Segments of this long bundle can be studied as a P1 crystal with a unit cell containing an acrosomal filament with 28 actin and 28 scruin molecules in 13 helical turns. A novel computational procedure was developed to extract single columns of superimposed acrosomal filaments from the distinctive crystallographic view. Helical reconstruction was used to generate a 3D structure of this computationally isolated acrosomal filament. The scruin molecule is organized into two domains which contact two actin subunits in different strands of the same actin filament. A correlation of Holmes' actin filament model to the density in our acrosomal filament map shows that actin subdomains 1, 2 and 3 match the model density closely. However, actin subdomain 4 matches rather poorly, suggesting that interactions with scruin may have altered actin conformation. Scruin makes extensive interactions with helix–loop–beta motifs in subdomain 3 of one actin subunit and in subdomain 1 of a consecutive actin subunit along the genetic filament helix. These two actin subdomains are structurally homologous and are closely spaced along the actin filament. Our model suggests that scruin, which is derived from a tandemly duplicated gene, has evolved to bind structurally homologous but non–identical positions across two consecutive actin subunits.

Acknowledgement: We thank NCRR/NIH and W.M. Keck Foundation for support.

Th-AM-B4

FILAMENTOUS HEMAGGLUTININ OF BORDETELLA PERTUSSIS: MONOMERIC HAIRPIN MODEL OF A BACTERIAL ADHESIN

((A. Makhov[1], J. Hannah[2], M. Brennan[2], B. Trus[1,3], E. Kocsis[1], J. Conway[1], P. Wingfield[4], M. Simon[5], and A. Steven[1])) [1] NIAMS-NIH; [2] DBP-FDA; [3] DCRT-NIH; [4] OD-NIH, Bethesda, MD 20892; and [5] Brookhaven Nat'l. Lab., Upton, NY 11973.

Filamentous hemagglutinin (FHA) binds B. pertussis cells to the respiratory epithelium in whooping-cough infections. Mature FHA is a 220-kDa secretory protein that is highly immunogenic, and has been included in acellular vaccines. We have combined electron microscopy with computational analysis of its amino-acid sequence to investigated its structure. Our analysis depicts a 50nm-long molecule with the morphology of a horseshoe nail: it has a globular head, which appears to consist of two domains; a 37nm-long shaft that averages 4nm in width; and a small, flexible, tail. Mass measurements by scanning transmission electron microscopy establish that FHA is a monomer. Its sequence contains two regions of tandem 19-residue pseudo-repeats: the first, of 38 cycles, starts at residue 343; the second, of 13 cycles, starts at residue 1440. The repeat motif is predicted to consist of short β-strands separated by β-turns, and this secondary structure is consistent with CD measurements. We propose a hairpin model for FHA in which the head is composed of the terminal domains; the shaft consists mainly of the repeat regions conformed as amphipathic, hyper-elongated, β-sheets; and the tail is composed of the intervening sequence. This model suggests how functionally important binding sites and immunodominant epitopes are deployed: the RGD fibronectin-like binding site is assigned to the tail; the putative hemagglutination site forms part of the head; and immunodominant epitopes are associated with the head-proximal segment of the shaft.

Th-AM-B5

11 Å HELICAL RECONSTRUCTION OF BACTERIAL FLAGELLIN ((D. Morgan, L. Melanson, T. Ruiz, and D.J. DeRosier)) Brandeis University, Waltham, MA 02254

The filament or propellor is the major extracellular constituent of the bacterial flagellum. In Salmonella typhimurium, the filament is composed of up to 20,000 copies of a single protein (flagellin). Biophysical and biochemical evidence indicates that the polymerization of flagellin into its helical assembly involves the formation of α-helical domains and that these new domains involve the N- and C-termini of flagellin. Early X-ray diffraction studies indicated there are bundles of α-helices running parallel to the filament axis. Recent advances in the automated analysis of electron micrographs of frozen-hydrated bacterial filaments have allowed us to reconstruct this assembly at a resolution of ~11 Å. We see rod-like features surrounding a 25 Å diameter channel at the center of the structure, and interpret these features as columns of individual α-helices stacked end to end. These columns run parallel to the helix axis and are tightly packed against each other to form a set of concentric tubes. The wall of the innermost tube, at a radius of ~20 Å, is formed from 11 columns. At a radius of ~40 Å is a second tube whose wall consists of 22 columns. The two concentric tubes are held apart by short segments of α-helix which act as spacers or shims. According to the helical symmetry of the filament, each flagellin subunit contributes 1 α-helix to the inner tube, 2 to the outer tube and 1 to the shims.

Th-AM-B6

EVIDENCE FOR CONFORMATIONAL DRIFT IN THE INTERACTION OF ANTIBODIES WITH HAPTENS. ((S.Y. Tetin, E.W .Voss, Jr. & T.L. Hazlett*)). Univ. of Illinois at U-C, Dept. Microbiology & *Dept. Physics, Laboratory for Fluorescence Dynamics, Urbana, Il 61801.

The binding equilibria of anti-fluorescein antibodies within the same idiotypic family: 4-4-20 (IgG2a,K); 9-40 (IgG1,K) and 5-27 (IgG1,K) were investigated with fluorescein and an analogue 6-hydroxy-9-phenylfluoron (HPF). At each point in the binding titration the concentration of complex was determined using various fluorescence measurements: fluorescence quenching, fluorescence anisotropy and fluorescence lifetime analyses. The antibody and fluorescein binding plots did not fit well with a simple binding model as would be expected for an antibody-hapten equilibrium. Stoichiometric binding of fluorescein to IgG 4-4-20 was experimentally verified, excluding more complicated cooperative binding models which might explain the data. In addition, comparing results with IgG 4-4-20 and a single-site 4-4-20 construct (SCA 4-4-20), we eliminated the possibility of interactions between binding sites on the same IgG molecule. The fluorescein binding data can, however, be fit well with a binding model based on a ligand-induced conformational drift. The principal point of this model is that the conformationally drifted protein has a slow relaxation after ligand release and therefore it persists in solution. Analysis of the binding data of all three antibodies with the conformational drift model, a free energy difference between the normal and drifted protein states, ΔG_{Loss}, was found to range from four to one RT units. Under similar conditions, in binding experiments with HPF, ΔG_{Loss} was reduced for IgG 4-4-20 and absent for IgG 9-40. This result indicates that the ΔG_{Loss} is dependent on the specific protein and ligand pair. At present the data suggest a working model for antibody-hapten interactions which includes a metastable drifted form of the protein induced by the ligand. Support; RR03155.

Th-AM-B7

CHIMERIC BISPECIFIC ANTIBODY BINDING SITES (χBABS): DESIGN OF A SECOND COMBINING SITE WITHIN THE Fv REGION & RECOVERY OF SINGLE-CHAIN Fv BINDING ACTIVITY AFTER INTEGRATION OF NEW BINDING LOOPS BETWEEN ß-STRANDS OF V DOMAINS. P.C. Keck, M.-S. Tai, H. Oppermann, & J.S. Huston. Creative BioMolecules, Inc., 45 South Street, Hopkinton, MA 01748.

A complete antibody combining site is formed by the Fv region, which is comprised of separate VH and VL domains. We report here that it is theoretically and empirically possible to build a second binding site diametrically opposite to the normal combining site, on the bottom concave surface of the isolated Fv. The ß-barrel symmetry of the Fv region allows complementarity-determining residues (CDRs) to be appropriately introduced between ß-strands. Molecular modeling indicated that the H1, H3, L1, and L3 CDR loops may be incorporated in a manner that maintains proper chain continuity, utilizes fixed end points, and replicates their normal relative positions. H2 and L2 loops may be oriented properly if added at the end of each V region, e.g. an H2 loop could bridge the C-terminal end of the VH and the interdomain linker of a single-chain χFv (χVH-VL). The anti-digoxin 26-10 single-chain Fv (Huston, *et al.*, PNAS 85, 5879-5883) has been used as a model for χBABS design. The H1, H2, and H3 loops from another antibody were genetically built into 26-10 sFv. After refolding, the χsFv bound to ouabain-Sepharose and eluted monomers were compactly folded. [Partly supported by SBIR grant #1 R43 CA52323-01 from NIH].

Th-AM-B8

MOLECULAR BASIS FOR THE MODULATED RECEPTOR AND MODE MODELS.

((Pal L. Vaghy)) Department of Medical Biochemistry, The Ohio Sate University, College of Medicine, Columbus, Ohio 43210-1218.

Two apparently different models are favored to explain complex binding and effects of drugs on voltage-dependent ion channels. The modulated receptor model suggests that binding and effects of drugs are conformation-dependent. The mode model suggests that drug act by promoting a naturally existing mode of gating. We suggest that drugs are multivalent ligands and can bind to one or two receptor subsites in the channel pore depending on the channel conformation. Binding to two subsites results in reversible cross-linking of neighboring peptide segments of the channel and stabilization of a naturally existing channel conformation. We have identified putative subsites of the dihydropyridine receptor on linker regions between S5 and S6 transmembrane segments in motifs I, III, and IV of the skeltal muscle L-type calcium channel. These segments are far away from each other in the primary structure of the receptor but must be close to each other when folded into the mouth of the channel and line the pore. If putative receptor subsites have different steric orientation in open and closed channel states, cross-linking by a channel inhibitor occurs when the subsites are within reach of two functional groups of a channel inhibitor, i.e. in a closed (inactivated) channel state. (Supported by NIH grant RO1 HL-41088.).

Th-AM-B9

EQUILIBRIUM Ca^{2+} TITRATIONS OF CALMODULIN MONITORED BY NMR.

((S. Pedigo and M. A. Shea)) Dept. of Biochemistry, Univ. of Iowa College of Medicine, Iowa City, IA 52242-1109

Calmodulin (CaM) is the primary eukaryotic intracellular Ca^{2+} receptor. When Ca^{2+} levels rise in response to signaling events, CaM binds up to four Ca^{2+} cooperatively. To identify the intermediate states populated during Ca^{2+} activation of CaM, we are developing techniques to monitor individual Ca^{2+}-binding sites and other positions at partial degrees of saturation. Previously, we have described the use of proteases to probe ligand-linked conformational changes of CaM by quantifying changes in proteolytic sensitivity of the protein backbone. In these experiments, we used 1D-proton NMR spectroscopy to monitor *equilibrium* Ca^{2+}-binding properties of CaM. Resonances arising from residues in the N-terminal and C-terminal domains behaved as distinct classes. N-terminal resonances shifted position as a function of Ca^{2+} concentration. This fast exchange behavior is indicative of weak Ca^{2+}-binding affinities in the N-terminal domain. In contrast, C-terminal domain resonances demonstrated slow exchange behavior in that they diminished or appeared over the course of the titration. This slow exchange behavior corroborates that the higher affinity Ca^{2+}-binding sites are in the C-terminal domain and that a slow conformational change occurs upon binding. These experiments explored the dependence of the Ca^{2+}-binding affinity of the sites on the concentration of KCl. Results from these titrations monitored by NMR spectroscopy are compared to proteolytically probed of CaM. NMR spectroscopy has proven useful for monitoring microscopic binding events in CaM under *equilibrium* binding conditions.

(NSF MCB 9057157, AHA 91014980, PHS 1 T32 GM08365-04)

Th-AM-B10

MECHANISM OF LANTHANIDE ION BINDING TO AN EF-HAND CALCIUM-BINDING DOMAIN ANALOGUE PEPTIDE.

((S. L. Helgerson[1], J. Bruno[2], J. E. Curtis[1], and W. D. Horrocks, Jr.[2])) [1]Baxter Biotech Group, Duarte, CA 91010 and [2]Department of Chemistry, The Pennsylvania State University, University Park, PA 16802.

Synthetic peptides based on the EF-hand domains from calcium-binding proteins are useful models for studying metal ion binding mechanisms. A typical calcium-binding loop consists of 12 residues that coordinate the metal ion using side chain or backbone carbonyl oxygen atoms. We have designed and synthesized a 33-residue peptide which includes an EF-hand loop sequence (residues #12-23) that is analogous to the EF calcium-binding loop of parvalbumin (residues #90-101). The residues at the coordinating positions are shown in capitals.

...*trp*-ASP_{12}-ser-ASP-gly-ASP-gly-LYS-Ile-gly-thr-asp-GLU_{23}-leu...

A single *trp* residue was placed prior to the binding loop to provide a spectroscopic probe for monitoring metal ion binding and conformational changes in the peptide. La^{3+} binding to the peptide results in a ~40% increase of the *trp* fluorescence emission intensity and in the appearance of positive CD bands at 272, 280, and 290nm. In contrast, Tb^{3+} or Eu^{3+} binding quench the fluorescence emission intensity by ~25% or ~65%, respectively. The laser-induced $^7F_0 \rightarrow {}^5D_0$ excitation spectrum of peptide-bound Eu^{3+} ion indicates that three distinct environments are present. Measurement of biexponential Eu^{3+} excited-state decays in H_2O and D_2O solutions indicate the presence of Eu^{3+} ions with 2.5 and 5 water molecules in the first coordination sphere. A titration based on the amplitudes of the component exponentials reveals two classes of binding site exist (K_D's ~0.1 and 4 μM). The observation that the Eu^{3+} excited-state lifetime is shortened by the presence of Nd^{3+} suggests the formation of a dimeric peptide species similar to that observed for the binding site III peptide derived from troponin C [Shaw *et al. Science 249*: 280-283 (1990)].

Supported by Baxter Healthcare Corp. (SLH, JEC) and NIH Grant GM 23599 (WDH).

K CHANNEL MODULATION

Th-AM-C1

THE INACTIVATION GATE OF A HUMAN A-TYPE K^+ CHANNEL IS MODULATED BY PROTEIN PHOSPHORYLATION.

((M. Covarrubias[1], A. Wei[2], T.B. Vyas[1] and L. Salkoff[2])) 1) Jefferson Medical College, Philadelphia, PA 19107 and 2) Washington University School of Medicine, St. Louis, MO 63110.

Rapid inactivation (τ=10 ms at +40 mV) of a human A-type K^+ channel (*hkv3.4*) was selectively reduced by activation of protein kinase C (PKC) in *Xenopus* oocytes. This could be due to phosphorylation of the inactivation gate at the N-terminus of the channel polypeptide. Three putative PKC phosphorylation sites are found in this region: Ser^{15}, Ser^{21} and Thr^{23}. To investigate their role, three sets of mutations were created: Ser^{15}Ala, Ser^{15}Ala/Ser^{21}Ala, and Ser^{21}Ala/Thr^{23}Ala. Ser^{15} accounts for ~50% of PKC action and, Ser^{21} and Thr^{23} account for approximately an additional 25%, each. These results strongly suggest that the inactivation gate in a human K^+ channel is directly regulated by PKC-mediated phosphorylation.

Supported by NIAAA to M.C. and NIH to L.S.

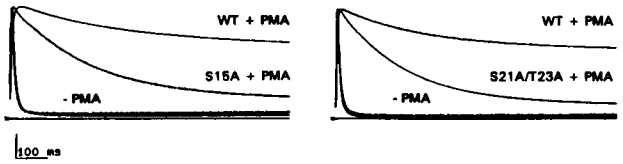

Th-AM-C2

CHARGED RESIDUES AT THE EXTERNAL TEA-BINDING SITE OF MAMMALIAN, VOLTAGE-GATED, *SHAKER*-RELATED POTASSIUM CHANNELS ALONE CANNOT ACCOUNT FOR THE MODULATORY EFFECT OF EXTRACELLULAR POTASSIUM.

((S. Grissmer, A.N. Nguyen, J. Aiyar and K.G. Chandy)). Department of Physiology and Biophysics. University of California, Irvine, CA 92717.

Using whole-cell recordings from cell lines stably expressing cloned wild type K^+ channels (Kv1.1, Kv1.2, Kv1.3, Kv1.5), or outside-out patch recordings from oocytes injected with cRNA for wild type (Kv1.3 and Kv1.4) and mutant K^+ channels (Kv1.3 H404R), we have studied the effect of removing extracellular potassium, ($[K^+]_o$), on the currents flowing through the different channel gene products. Whole-cell currents were elicited with 50 or 200 ms voltage steps from -80 mV to 40 mV in the presence (4.5 mM) and absence of $[K^+]_o$. Pardo *et al.* (*PNAS* 89:2466-2470, 1992) hypothesized that positively charged residues at the TEA-binding site in voltage-gated *Shaker*-related K^+ channels are involved in the regulation by $[K^+]_o$. In accordance with this hypothesis was our observation that a) currents through Kv1.1 and Kv1.2 with uncharged residues at the TEA-binding site (tyrosine in Kv1.1; valine in Kv1.2) were insensitive to a change in $[K^+]_o$; b) currents through Kv1.3 with a partially charged residue at the TEA-binding site (histidine) was sensitive to $[K^+]_o$ in a pH dependent way; c) replacing the histidine in Kv1.3 with arginine resulted in an absolute requirement for the presence of $[K^+]_o$ even at normal pH 7.4; d) current through Kv1.4 with a positively charged residue (lysine) was very sensitive to a change in $[K^+]_o$. Several observations, however, are inconsistent with this hypothesis; a) current through Kv1.5 with a positively charged arginine was only marginally sensitive to a change in $[K^+]_o$ at pH 7.4; b) at pH 6.0 current through Kv1.5 became extremely sensitive to $[K^+]_o$ indicating that other titratetable residues might play important roles in determining the sensitivity to $[K^+]_o$. One possible candidate, a histidine between S5 and the "P"-region, was ruled out since Kv1.1 also has a histidine in that position but did not show any sensitivity to $[K^+]_o$ even at low pH.

Supported by grants from Pfizer Inc., Groton, CT (KGC), and from Pfizer Ltd., Sandwich, UK (SG).

Th-AM-C3

MODULATION OF *SLO* K_{Ca} CHANNELS BY PHOSPHORYLATION IN LIPID BILAYERS.

((G. Pérez*, M. Ottolia*, A. Lagrutta§, J. Adelman§, and L. Toro*)) *Baylor College of Medicine, Houston, TX 77030. §Oregon Health Sc. Univ. Portland, OR 97201.

Membrane vesicles from *Xenopus* oocytes expressing K_{Ca} channels were isolated and reconstituted into lipid bilayers. The reconstituted channels demonstrate functional properties characteristic of native K_{Ca} channels. They possess a unitary conductance of 220 ± 10 pS (n=11) in symmetrical potassium (250 mM). At 50 µM $[Ca^{2+}]i$, K_{Ca} channels were half activated at -20 ± 1 mV, and had a calculated effective valence of near 1 (0.94 ± 0.6, n=10). Reconstituted *Slo* K_{Ca} channels were insensitive to charybdotoxin (40-200 nM), and sensitive to micromolar concentrations of external tetraethylammonium (K_D = 158 µM, at 0 mV) and internal Ba^{2+} (K_D = 76 µM, at 40 mV). In addition, they were blocked by internally applied "ball" inactivating peptide (K_D = 480 µM, at 40 mV). Reconstituted *Slo* K_{Ca} channels also respond to protein kinase A-dependent phosphorylation as their mammalian counterparts. Internal addition of 20-40 U/ml catalytic subunit of PKA in the presence of 0.5-1 mM ATP-Mg can diminish channel open probability from 0.58 ± 0.13 to 0.28 ± 0.08 (n=4). This inhibition could be partially restored after addition of 80 U/ml of alkaline phosphatase (Po = 0.4 ± 0.07, n=2). These results demonstrate that K_{Ca} channels expressed in *Xenopus* oocytes can be readily studied after being incorporated into lipid bilayers, that similar binding sites for TEA, Ba^{2+}, and "ball" inactivating peptide have been conserved through evolution, and that *Slo* K_{Ca} channels can be modulated by phosphorylation as their mammalian counterparts.

Supported by NIH grants HL47382, HL37044, NS28504.

Th-AM-C4

Gs PROTEIN ACTIVATION OF A PURIFIED K_{Ca} CHANNEL RECONSTITUTED IN LIPID BILAYERS.

((F.S. Scornik*, J. Codina*, M. García-Calvo§, M.-G. Kraus§, L. Birnbaumer*, M. L. García§ and L. Toro*)) *Baylor College of Medicine, Houston, TX 77030. §Merck Res. Labs. Rahway, NJ 07065.

Large conductance calcium-activated potassium (K_{Ca}) channels from coronary smooth muscle incorporated into bilayers are activated by GTPγS and by the activated α subunit of the G_s (α_s*) protein (Scornik *et al.*, AJP, 1993), suggesting that Gs protein may directly interact with the channel protein itself or with a closely associated molecule. In an attempt to differentiate between these two possibilities we have studied the action of α_s* on a purified K_{Ca} channel from tracheal smooth muscle (García-Calvo, *et al.*, JBC, in press). K_{Ca} channels from two different purifications were studied. After incorporation into lipid bilayers, only liposomes containing the purified charybdotoxin receptor, but not other proteins, induced K_{Ca} channel activity (≈200 pS, 250 KCl). Addition of 300 pM of purified α_s* to the intracellular side of purified K_{Ca} channels stimulated channel activity from Po 0.29 ± 0.07 to 0.45 ± 0.1 (n=6). Similar to the action of α_s* on native coronary K_{Ca} channels, α_s* induced a major effect on the closed state of the channel. Mean closed times decreased from 162 ± 76 ms to 71 ± 39 ms (n=5) after α_s* treatment, while mean open times remained practically unchanged (34 ± 8 ms vs. 39 ± 9 ms, n=5). As expected for a purified preparation devoid of endogenous G proteins, 100 µM GTPγS was unable to induce an increase in channel Po (0.24 ± 0.05 vs. 0.27 ± 0.06, n=8). The stimulatory action of α_s* on purified K_{Ca} channels seemed to be specific since internal application of either 7 nM βγ dimers or 300 pM boiled α_s* were unable to increase channel Po (n=8). These results are consistent with the idea that activation of K_{Ca} channels by Gs protein involves a direct interaction between the channel and the α subunit of Gs.

Supported by NIH (HL47382 to LT, DK19318 to LB).

Th-AM-C5

HETEROLOGOUS EXPRESSION OF THE βγ G PROTEIN SUBUNITS IS SUFFICIENT TO ACTIVATE THE MUSCARINIC POTASSIUM CHANNEL (GIRK1). ((E. Reuveny, P.A. Slesinger, Y.N. Jan and L.Y. Jan)). Howard Hughes Medical Institute, Univ. of Calif. Med. School. San Francisco, CA 94143.

Parasympathetic nerve stimulation causes slowing of the heart rate via activation of muscarinic receptors by opening muscarinic K^+ channels. We have recently cloned this G-protein coupled inwardly rectifying K^+ channel (GIRK1; Kubo et al., *Nature*, 1993). Previous studies examining the mechanism of activation have relied on exogenous application of recombinant or purified G protein subunits on native muscarinic channels and have suggested that both the α and βγ subunits are involved. With the cloning of GIRK1, it is now possible to examine the effect of heterologously expressed G protein subunits on the activation of the muscarinic K^+ channel. We have expressed the GIRK1 clone and the $\beta_1\gamma_2$ subunits in *Xenopus* oocytes with or without the α_{i2} subunit. Similar large inwardly rectifying macroscopic current were measured under two-electrode voltage clamp from oocytes injected with GIRK1, $\beta_1\gamma_2$ +/- α_{i2} subunit. Single channel recordings in the cell-attached mode also showed channels with similar conductance and rectification properties. However, excising patches into solution that minimized the activation of α_{i2} subunit (no GTP) showed a striking difference: channel activity was maintained for up to 30 minutes in oocytes injected with only $\beta_1\gamma_2$, but decreased rapidly in oocytes injected with $\beta_1\gamma_2$ plus the α_{i2} subunit. Sustained channel activity was also recorded with either GDPβS or a Mg^{2+}-free internal solution from oocytes injected with only $\beta_1\gamma_2$. These results suggest that βγ are sufficient to activate the muscarinic K^+ channel and that the role of the α subunit may be to terminate the activation by binding βγ. We are currently examining whether inactivating expressed βγ subunits by other means can reduce muscarinic K^+ channel activity.

Th-AM-C6

A POTASSIUM CHANNEL β-SUBUNIT FROM RAT BRAIN INDUCES N-TYPE INACTIVATION.

((Stefan H. Heinemann[1], Jens Rettig[2], Christoph Lorra[2], Olaf Pongs[2]))
1: Max-Planck-Insititut für biophysikalische Chemie, Abteilung Membranbiophysik, D-37077 Göttingen, Germany;
2: Zentrum für Molekulare Neurobiologie Hamburg, Institut für Neurale Signalverarbeitung, D-20246 Hamburg, Germany

A potassium channel β-subunit from rat brain was cloned and coexpressed with various potassium channel α-subunits. The β-subunit increased the speed of N-type inactivation of the A-type channels Kv1.4 and *Shaker* B. After deletion of the N-terminal regions of the α-subunits (Kv1.4Δ1-110 and *Sh*BΔ6-46), which remove fast channel inactivation, the β-subunit still induced fast channel inactivation. The same effect was observed with the delayed rectifyer channel Kv1.1. Deletion of the first 34 amino acids of the β-subunit (βΔ1-34) abolished its effect of channel inactivation when coexpressed with Kv1.4Δ1-110 suggesting that the β-subunit can contribute with its own N-terminus to the N-type inactivation of potassium channels. As observed fro N-type inactivation of Kv1.4, the β-induced inactivation is regulated by the intracellular redox potential. These results are consistent with the β-subunit of potassium channels as being associated with the α-subunits on the intracellular side. They modulate channel function by an additional N(β)-type inactivation which can be immobilized in oxidizing environments by disulphide bridges.

Th-AM-C7

G PROTEINS ACTIVATE ATP-SENSITIVE K^+ CHANNELS BY ANTAGONIZING THE ATP-DEPENDENT GATING.

((A. Terzic, R.T. Tung, A. Inanobe, T. Katada and Y. Kurachi)) Mayo Clinic, Rochester, MN, USA and University of Tokyo, Tokyo, Japan.

To identify the mechanism responsible for G protein activation of ATP-sensitive K^+ (K_{ATP}) channels, currents were measured in inside-out patches excised from cardiomyocytes. When ATP suppressed K_{ATP} channels, activators of endogenous G proteins, GTP (plus adenosine or acetylcholine in the pipette), GTPγS, or complexes of fluoride with aluminum (AlF_4^-) enhanced spontaneous K_{ATP} channel openings, an effect prevented by GDPβS, an antagonist of G protein activation. In the absence of ATP, however, G protein activators did not increase channel activity before, during, or after "run-down" of spontaneous channel activity. Nucleoside diphosphates (NDPs) restored K_{ATP} channel openings after the "run-down" of spontaneous activity. In the absence of ATP, G protein activators did not enhance NDP-induced K_{ATP} channel activity. However, when ATP suppressed NDP-induced channel openings, GTPγS or AlF_4^- enhanced K_{ATP} channel activity. Active forms of exogenous $G_{\alpha i}$-1, $G_{\alpha i}$-2, or $G_{\alpha o}$ subunits activated K_{ATP} channels closed by ATP, but were ineffective in the absence of ATP. Hence, G proteins stimulate either spontaneous or NDP-induced openings of cardiac K_{ATP} channels solely by antagonizing the ATP-dependent inhibitory gating of these channels.

Th-AM-C8

ROLE OF Mg2+ IN β CELL K_{ATP} CHANNEL MODULATION BY G PROTEINS. ((B. Ribalet and S. Ciani)) Dept.of Physiology, UCLA, Los Angeles, CA 90024.

In outside-out and cell-attached patches, HIT cell K_{ATP} channels are activated by 10 nM somatostatin and inhibited by 10 nM glucagon. In inside-out patches, the G protein α subunits, α_i or α_o stimulate K_{ATP} channel activity, while α_s has no effect, and βγ is inhibitory. These results are consistent with the following hypotheses: 1. K_{ATP} channel stimulation by activated G_i-coupled receptors (e.g. somatostatin) involves interaction of α_i with the channel; 2. K_{ATP} channel inhibition by activated G_s-coupled receptors (e.g. glucagon) results from the association of βγ (originating from G_s activation) with stimulatory α_i subunits. Such interactions between G protein subunits and the K channel may account for the modulation of channel activity by Mg^{2+}. In inside-out patches, bath concentrations of Mg^{2+} below 1 mM increase K_{ATP} channel activity while higher concentrations are inhibitory. In the presence of GTP, the activation of trimeric G proteins is Mg^{2+} dependent. Low concentrations of Mg^{2+} are sufficient to induce G_i dissociation, while higher concentrations are needed for dissociation of G_s. Based on these observations, we postulate that channel stimulation by low Mg^{2+} is due to G_i activation and thus elevation of α_i. Channel inhibition by higher Mg^{2+} levels may be due to the activation of G_s, the resulting liberation of βγ causing α_i to revert to an inactive trimeric form.

Th-AM-C9

PURIFICATION AND RECONSTITUTION OF FUNCTIONAL SHAKER K CHANNELS ASSAYED WITH A LIGHT-DRIVEN, VOLTAGE-CONTROL SYSTEM. ((L. Santacruz-Toloza, E. Perozo, and D.M. Papazian)) Department of Physiology and Jules Stein Eye Institute, UCLA School of Medicine, Los Angeles, CA 90024. (Spon. by D. Loo)

To facilitate structural studies of K channels, Shaker K channels have been purified from an insect expression system. Sf9 cells were infected with a recombinant baculovirus encoding Shaker protein. A membrane fraction was prepared and membrane proteins were solubilized with Lubrol-PX. Channel protein was purified using an immunoaffinity resin made from a Shaker antipeptide antibody. On silver-stained, SDS polyacrylamide gels, the material eluted with the peptide epitope was homogeneous and contained bands that were identified as Shaker protein on parallel immunoblots. The purified channels were reconstituted and assayed using a light-driven, vesicular voltage control system (Perozo & Hubbell, *Biochem.*, *32*: 10471-10478, 1993). Shaker-containing vesicles were fused with vesicles containing bacteriorhodopsin (bR) reconstituted in an inside-out orientation. Inactivation of Shaker channels was removed by the generation of a nitrate diffusion potential in the vesicles, inside negative. Upon illumination, proton pumping by bR depolarized the vesicles, activating only those Shaker channels oriented outside-out. Channel activity was detected as $^{86}Rb^+$ uptake, which was blockable by the K channel blockers TEA and Ba^{2+}. Using this assay, the purified Shaker K channels were shown to be functional. Purification of active protein is a prerequisite for structural analysis, since activity is the key indication that the structural integrity of the channel has survived biochemical manipulations. (Supported by the NIH (GM43459), the Klingenstein Fund, and the Pew Charitable Trusts.)

Th-AM-C10

PURIFICATION AND BIOCHEMICAL CHARACTERIZATION OF A MAMMALIAN K^+ CHANNEL PROTEIN, Kv1.3. ((R.H. Spencer*, B. Takenaka, J. Aiyar, A. Nguyen, S. Grissmer, G.A. Gutman*, and K.G. Chandy)) Dept. of Physiol. & Biophys. and *Dept. of Micro. & Mol. Genetics, UC Irvine, CA 92717

To generate adequate sources of homogeneous K^+ channel protein for biochemical and structural studies, we used a vaccinia viral system to express the Kv1.3 K^+ channel as a fusion protein, Kv1.3/His/G10. This construct contains a poly-histidine repeat (for Ni-chelate chromatography), a sequence from gene 10 of bacteriophage T7, and an enterokinase cleavage site, which adds an additional 37 amino acids to the N-terminus. The expression of this fusion protein in CV-1 cells produces channels which are biophysically identical to native Kv1.3. Whole cell currents of 100-400 nA per cell are attained, equivalent to $1\text{-}5\times10^5$ channels per cell. Solubilization of this protein (predicted mass = 62 kDa) from 10^7 cells followed by Ni-chelate chromatography yielded protein of >70% purity. FPLC gel filtration resulted in protein of ~90% purity (analyzed by silver stained gels) which eluted with a mass similar to β-amylase (200 kDa), suggesting that this protein may be assembled as a tetramer. We have also obtained evidence for glycosylation of the Kv1.3 protein. Immunoprecipitation of ^{35}S-Met-labeled Kv1.3 protein from several vaccinia-infected mammalian cell lines (CV-1, NIH-3T3, U937, RBL, Jurkat) in the presence or absence of tunicamycin, demonstrates a small, yet distinct shift in the apparent migration of the protein analyzed by SDS-PAGE. Tunicamycin treatment does not, however, alter any of the biophysical properties of the channel. Preliminary immunoprecipitation studies also show the existence of a phosphorylated form of Kv1.3. We are exploring the effects of kinase- and phosphatase-modulators on the phosphorylation of Kv1.3 in vaccinia-infected cells and its effect on ionic conductance. (Supported by grants from Pfizer, Inc., AI24783. and the Cancer Research Inst., UCI).

Th-AM-D1

PSEUDOSUBSTRATE REGULATION OF PROTEIN KINASE C

((Jeffrey W. Orr and Alexandra C. Newton))
Department of Chemistry, Indiana University, Bloomington, IN 47405

Protein kinase C is allosterically activated by diacylglycerol and phosphatidylserine. The enzyme is also activated by surprisingly dissimilar compounds such as short-chained phosphatidylcholines and protamine sulfate. Here we show that conventional and non-conventional activators of protein kinase C βII produce the same structural alteration: they expose Arg^{19} of the autoinhibitory pseudosubstrate domain to proteolysis. Molecular modeling of protein kinase C's catalytic domain, based on the structure of the cAMP-dependent kinase's catalytic domain, indicates that Arg^{19} is shielded by a cluster of acidic residues when the pseudosubstrate occupies the substrate-binding site. Our biochemical data and structural modeling indicate a common mechanism of intrapeptide regulation of protein kinase C by all activators that involves release of the pseudosubstrate from the active site.

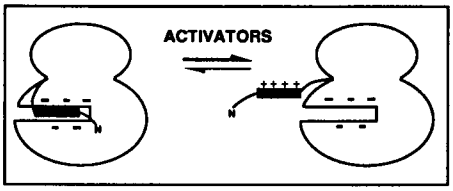

Th-AM-D2

INVOLVEMENT OF CA^{2+} IN THE COOPERATIVE BINDING OF PROTEIN KINASE C TO PHOSPHATIDYLSERINE

((Alexandra C. Newton, Kyle W. Uphoff, and Lisa M. Keranen))
Department of Chemistry, Indiana University, Bloomington, IN 47405

Protein kinase C is allosterically regulated by phosphatidylserine and diacylglycerol, two lipids that activate the enzyme by exposing its auto-inhibitory pseudosubstrate domain. For Ca^{2+}-regulated isozymes of protein kinase C, the interaction with phosphatidylserine displays high cooperativity in the presence of saturating Ca^{2+}. This contribution dissects out the role of Ca^{2+} in the cooperative binding and activation. We show that a Ca^{2+}-dependent isozyme of protein kinase C (βII) displays two distinct Ca^{2+} requirements: ≤μM Ca^{2+} promotes lipid-binding whereas two orders of magnitude more Ca^{2+} induces pseudosubstrate exposure and activation. Tb^{3+} replaces Ca^{2+} in the cation requirement for lipid-binding but cannot substitute for Ca^{2+} in activating the enzyme. These results suggest that protein kinase C βII has two Ca^{2+} binding sites: occupancy of the high affinity site promotes membrane-binding and occupancy of the lower affinity site promotes catalysis by reducing the affinity of the pseudosubstrate for the active site. In contrast, a Ca^{2+}-independent isozyme of protein kinase C (ε) cooperatively binds phosphatidyl-serine in the complete absence of Ca^{2+}. The binding of this enzyme to phosphatidylserine is regulated only by diacylglycerol. Thus, the cooperative interaction with phosphatidylserine does not arise because Ca^{2+} is altering the structure of membranes, but rather reflects an intrinsic property of the enzyme. The role of Ca^{2+} appears to be allosteric: it alters the structure of the Ca^{2+}-dependent protein kinase Cs so as to increase their affinity for lipid.

Th-AM-D3

CHARACTERIZATION OF Ca^{2+}-BINDING SITE REGULATING THE ASSOCIATION OF PROTEIN KINASE C WITH PHOSPHOLIPID BILAYER.

((M. Mosior and R. M. Epand)) Department of Biochemistry, McMaster University, Hamilton, Ontario, Canada L8N 3Z5

Classic isotypes of protein kinase C (PKC) require Ca^{2+} for both the binding of the enzyme to the phospholipid bilayer and its subsequent activation. Using a sucrose-loaded vesicle assay, we have determined the functional stoichiometry of the Ca^{2+}-PKC-membrane complex, the affinity of Ca^{2+}-binding site, and its localization with respect to the membrane surface. The linear dependence of PKC binding to the membrane implicates a single Ca^{2+}-binding site for regulation of the association of the enzyme with the lipid bilayer. The apparent dissociation constant of Ca^{2+} or the protein-membrane complex depends on the double-layer potential produced by acidic lipids. Application of the Gouy-Chapman theory of the double-layer potential and the Boltzmann equation to the calculation of Ca^{2+} distribution in the proximity of the membrane surface yielded a unique value of 600 nM as the dissociation constant of Ca^{2+} from the putative binding site located about 0.3 nm from the interface. The apparent saturation of the dependence of PKC on Ca^{2+} concentration in the milimolar range indicated that this ion may also bind to the soluble form of the enzyme with a dissociation constant of about 3 mM. The ratio of the dissociation constants of Ca^{2+} from the soluble and membrane-bound PKC yields a value of 5 kcal/mol as an estimate of the free energy change of the conformational transition from the soluble to membrane-bound state.

Th-AM-D4

HYPOXIA DECREASES BRAIN CREATINE KINASE REACTION RATE IN VIVO. ((M.Tsuji, H.Naruse, D.Holtzman)) Depts. Neurology & Medicine, Children's Hospital, Boston, MA 02115 (Spons. D. Kirschner).

Cellular hypoxia, due to cyanide, has a two phase effect on the creatine kinase (CK) catalyzed reaction in mouse brain (Holtzman et al., J. Cereb. Blood Flow Metab. 13:153-161, 1993). The reaction rate increases at low doses and decreases at high doses. We now report decreased brain CK reaction rates after hypoxemia in 4 week old piglets. Anesthetized ventilated piglets were exposed to successive 10 min periods of increasing hypoxia (12%, 8%, 6%, 4% O2) with full recovery between hypoxic periods. Arterial blood pressure, heart rate and blood gasses were measured. Changes in brain oxygenated and deoxygenated hemoglobin, blood volume, and cytochrome aa3 (cytaa3) oxidation/reduction state were measured with near infra-red spectroscopy. Phosphocreatine (PCr), ATP, and pH were measured every 2 min during and after the hypoxic periods using 31P-NMR spectroscopy. After recovery from the hypoxic changes, the CK reaction rate was measured using the steady state saturation transfer NMR experiment. With mild hypoxia the cytaa3 signal became more oxidized and blood volume increased. Loss of PCr and ATP occurred only after the cytaa3 signal became more reduced than at baseline. The CK reaction rate was significantly decreased after each hypoxic period (e.g., 12% O2, 72±24% mean±SD of prehypoxia rate, $p < .02$; after all hypoxic periods, 73±26%, $p < .0001$). In all animals, the CK reaction rate decreased before reduction of cytaa3 and altered CK reactant concentrations. CONCLUSION: The CK reaction rate in vivo decreases at inspired O2 concentrations which produce no loss of cellular energy in hypoxic brain. (Supported by the Cerebral Palsy Foundation and NINDS).

Th-AM-D5

CONFORMATIONAL CHANGES ACCOMPANYING CALCINEURIN SUBUNIT ASSOCIATION AND THE EFFECT OF CALCINEURIN B MYRISTOYLATION. ((F. Rusnak, A. Haddy, R. Sikkink & M. Kennedy)) Mayo Graduate School of Medicine, Rochester, MN 55905.

The association of subunits of the protein phosphatase calcineurin into the native heterodimer has been investigated using gel filtration chromatography and analyses of enzyme activity. The catalytic calcineurin A (CNA) subunit could be reconstituted with myristoylated (myrCNB) as well as non-myristoylated (nCNB) calcineurin B subunit and purified to homogeneity using affinity and gel filtration chromatographies. The reconstituted heterodimers chromatographed with indistinguishable molecular masses of ≈78 kDa, consistent with a native-like one-to-one CNA/CNB ratio. In contrast, isolated CNA subunit chromatographed with an anomalously large molecular mass ≥ 1.5 MDa. These results suggest that CNB induces a conformational change in the catalytic subunit and may assist in protein folding and native subunit assembly. Additional conformational changes in the B subunit upon myristoylation and binding of Ca(II) were observed by electrophoresis under denaturing conditions and gel filtration chromatography, respectively. CNA p-nitrophenylphosphatase activity was stimulated appreciably (≥10-fold) by both myrCNB and nCNB although the myristoylated heterodimer had a 2-fold higher activity versus enzyme reconstituted with nCNB. Analyses during the course of purification demonstrated that CNB myristoylation did not affect the yield of reconstituted heterodimer. These results indicate that although myristoylation led to noticeable structural changes in CNB and small differences in holoenzyme activity, fatty acid modification itself does not appear to affect subunit association.

Th-AM-D6

EFFECT OF ENVIRONMENTAL CONDITIONS ON RADIATION TARGET SIZE ANALYSES. ((E. S. Kempner and J. H. Miller)) NIAMS, NIH, Bethesda MD 20892

Target analysis is an important adjunct in the determination of molecular mass of biologically active molecules. Results are dependent on the physical and chemical environment of the sample during radiation exposure. Effects of temperature and physical state have already been described. Buffers, protein concentration and the addition of small molecules are examined for several enzymes. Phosphate buffer is found to have major effects on the rate of inactivation of certain, but not all, proteins. The amount of protein in irradiated samples is significant for all enzymes studied, and the appropriate target size is obtained only at protein concentrations >2 mg/ml. The nature of the specific protein used is unimportant. Neither sucrose nor other glycitols could substitute for protein in target size determinations. Certain small molecules, especially cysteamine, were effective in sparing the need for high protein levels in radiation inactivation studies of four enzyme systems. The competent small molecules all are free radical scavengers, suggesting a limited role for free radicals in the radiation inactivation of proteins at low concentrations.

Th-AM-D7

STRUCTURE OF THE TRYPTOPHAN TRYPTOPHYL-SEMIQUINONE CATALYTIC INTERMEDIATE IN METHYLAMINE DEHYDROGENASE.
((K. Warncke, H. B. Brooks†, H.-I. Lee, G.T. Babcock, V. L. Davidson†, & J. McCracken)) Dept. of Chemistry, Michigan State Univ., East Lansing, MI 48824 & †Dept. of Biochemistry, Univ. of Mississippi Medical Center, Jackson, MS 39216

Methylamine dehydrogenase (MADH) catalyzes the oxidation of primary amines to the corresponding aldehydes with production of two reducing equivalents and ammonia. The active site cofactor is tryptophan tryptophylquinone (TTQ), a 2-4' covalently-linked dimer of tryptophan sidechains in which one indole group incorporates a 6'-7' *o*-quinone function. To gain insight into nuclear and electronic structural factors governing catalysis, we have compared results from combined X-band EPR, ^{1}H electron-nuclear double resonance (ENDOR) and multifrequency- (8.8-13.7 GHz) electron spin echo envelope modulation (ESEEM) spectroscopic studies of the following two TTQ-derived semiquinone species in MADH isolated from *Paracoccus denitrificans*: a) the native catalytic intermediate formed following one electron oxidation of methylamine-reduced enzyme (in which we have shown covalent substrate nitrogen bonding, *J. Am. Chem. Soc.* 1993, *115*, 6464), and b) the semiquinone formed by direct reduction with dithionite. Weak ^{2}H ESEEM from enzyme dithionite-reduced in $^{2}H_{2}O$ indicates that unpaired spin density is well-sequestered from solvent nuclei; the absence of distinct ^{2}H hyperfine coupling (hfc) suggests that the oxygen atoms are deprotonated. Simulations of strong ESEEM observed from two ^{14}N nuclei yield nuclear quadrupole coupling constants and asymmetry parameters consistent with indole nitrogen. One nitrogen (N2) is characterized by larger hyperfine anisotropy and displays quadrupole parameters perturbed from indole relative to the other nitrogen (N1) and is thus assigned to the modified indolyl moiety. Comparison of spectra from ^{14}N- and ^{15}N- methylamine- *vs.* dithionite- reduced enzyme reveals the following: a) the peak-trough EPR linewidth is broadened by 3 gauss, b) the amplitude of N2 ESEEM features is decreased severely while N1 features are only perturbed subtley , and c) there are selective changes in intensity and position of some of the 10 non-exchangeable and ≥2 exchangeable ^{1}H hfcs observed by ENDOR. These results reveal that the distribution of unpaired spin density is responsive to structural changes at the active carbon center, suggesting that bond-making/breaking can be coupled to changes in electronic structure that may influence the electron transfers involving the semiquinone. Support: NIH GM-41574 (V.L.D), GM-37300 (G.T.B.), GM-45795 (J.M.)

Th-AM-D8

"SECONDARY" BINDING SITES OF ACETYLCHOLINE IN THE AROMATIC GORGE LEADING TO THE ACTIVE SITE OF ACETYLCHOLINESTERASE.
((A. PULLMAN and X. HUI)) Institut de Biologie Physico-Chimique, 13, rue Pierre et Marie Curie, 75005 Paris, France.

Added to the large amount of evidence accumulated in recent years on the role of aromatic residues in the binding of alkylammonium ion derivatives to proteins, the observation of the presence of 14 aromatics along the walls of the deep and narrow gorge leading to the active site of acetylcholinesterase (ACHE) has led to the intriguing hypothesis that the substrate "uses the aromatic surface of the gorge to slide down to the bottom via a series of low-affinity sites" (J. Sussman and I. Silman, Current Opinions in Structural Biology, 1992, 2, 721-729). In view of characterizing the existence, if any, and energetics of such sites, we have performed calculations by energy-optimization techniques of the interactions of acetylcholine (ACH) with the gorge using the X-ray coordinates of the 14 aromatic amino acids Y70, 121, 130, 334, 342, F288, 290, 330, 331, W84, 114, 233, 279, 432, the anionic residues D72, 285, E199, 273, and the active site S200, E327, H440, plus A201 and G202.

Using a large number of starting positions of the substrate, the molecule was allowed in each case to optimize its conformation and position inside the gorge frozen. Examination of the ensemble of local minima obtained indicate the existence of "binding sites" or rather "sites of favorable interactions", as well as their relative strengths, and the role in them of the aromatics and/or of the charged residues present. The energies improve in a definite pattern from top to bottom towards a cluster of very similar values close to the binding site. The role of the anionic residues along the path and close to the site will be discussed.

Th-AM-D9

HETEROTROPIC ALLOSTERY IN ASPARTATE TRANSCARBAMYLASE: KINETIC AND THERMODYNAMIC STUDIES
((Vince J. LiCata, Anna M. Vu, and Norma M. Allewell)) Department of Biochemistry, University of Minnesota, St. Paul, MN 55108

E. coli aspartate transcarbamylase (ATCase) catalyzes the first committed step in pyrimidine biosynthesis, the condensation of aspartate and carbamyl phosphate. ATCase is allosterically up-regulated by ATP and down-regulated by pyrimidine nucleotides (CTP, UTP, and dTTP). We are pursuing a strategy of using solution effects to address questions about the mechanism of heterotropic allostery at the molecular level. We have studied the dependency of the enzyme activity of ATCase on [NaCl] and temperature in the presence and absence of allosteric effectors and found that: 1) Regulation of aspartate binding by CTP appears to involve the breaking of a net "extra" ionic bond relative to regulation by ATP or in the absence of effectors. (2) There appear to be different electrostatic "pathways" for regulation of V_{max} and K_{m}. 3) Aspartate binding is enthalpy driven in the presence and absence of allosteric effectors; positive (ATP) versus negative (CTP) heterotropic regulation occurs by "fine tuning" the enthalpy-entropy compensation for binding aspartate. 4) An equation which incorporates a Hill coefficient into an un-competitive model for substrate inhibition fits the kinetic data and returns physically meaningful values for all parameters. 5) Preliminary experiments suggest that TTP acts as a negative allosteric effector of ATCase and that cooperative effects between CTP and TTP, and between CTP and UTP, are pH dependent.
Supported by NIH grant DK-17335 (to NMA) and F32-GM14400 (to VJL)

Th-AM-D10

MECHANISTIC STUDIES OF TRIOSE PHOSPHATE ISOMERASE BY SOLID STATE NMR
((A. Cohen, T. Gu, A. McDermott, Y. Tomita, E. J. O'Connor, T. Polenova, J. Williams)) Columbia University, Department of Chemistry NY NY 10027 (Sponsored by A. McDermott)

We have used several solid-state NMR methods to probe the structure and dynamics of complexes of Triose Phosphate Isomerase (TIM) with substrate analog or transition state analog (TSA) compounds.

^{13}C chemical shielding anisotropy (CSA) analysis shows clearly that the TSA phosphoglycolic acid (PGA) is deprotonated and involved in strong hydrogen bonds as it is bound on TIM. This conclusion is based on an extensive database of carboxyl -containing model compounds with NMR, IR and structural analyses. The NMR results on PGA support the idea that it is a mimic for the charge build-up on the carbonyl at the transition state or in the intermediates of the reaction.

Rotational resonance (RR), a method previously used to measure internuclear distances, was used here to measure a dihedral angle about the C-C bond in doubly ^{13}C labeled PGA bound to TIM. We have studied the utility of RR for measuring dihedral angles in a variety of structurally-characterized doubly-labeled compounds. The data on PGA bound to TIM address a hypothesis about the stereoelectronic control of reactivity by the conformation of the enediol intermediate on TIM.

Deuterium broadline NMR was used to measure the rates and populations for the open-to-closed transition of a flexible loop in TIM, and we compared these rates for samples with and without substrate or transition state analog compound bound. We found that, unlike a ligand-gated-transition model, the motion in the TIM loop is comparable with and without the substrate analog present, with a rate slightly faster than the enzyme turnover rate. In addition, this motion actually slows down upon binding of the transition state analog. We interpret these data to indicate that the enzyme must access the open and closed states when empty and also when a product or substrate is bound so that substrate binding and product release are not rate limiting. However it should not access the open state when the transition state is formed.

STRUCTURALLY AND FUNCTIONALLY SPECIFIC WATER

Th-AM-SymII-1

The Role of Fixed Water Sites in Specific Protein-Nucleic Acid Interaction.
Paul B. Sigler, Dept. of Molec. Biophysics & Biochemistry, Yale University

Th-AM-SymII-2

DNA HYDRATION IN HIGH RESOLUTION CRYSTAL STRUCTURES AND ITS IMPLICATIONS FOR DNA-PROTEIN INTERACTIONS.
Zippora Shakked, Structural Chemistry Dept., Weizmann Institute, Rehovot 76100 Israel

Th-AM-SymII-3

Hydration in Solution and Protein Surface Structure.
Kurt Wuthrich, ETH, Zurich, Switzerland

Th-AM-SymII-4

BINDING SITE WATER MOLECULES MODULATE THE SPECIFICITY AND AFFINITY OF A PROTEIN INVOLVED IN SUGAR TRANSPORT.
((Florante A. Quiocho)) HOWARD HUGHES MEDICAL INSTITUTE AND BAYLOR COLLEGE OF MEDICINE, Houston, TX 77030.

The periplasmic L-arabinose-binding protein (ABP) of Gram-negative bacteria serves as an initial high affinity receptor for active transport or permease system. ABP binds L-arabinose, D-galactose and D-fucose with K_d values of 0.098, 0.23, and 3.8 μM, respectively. Thus the substitution of one of the H atoms at the C5 of L-arabinose with $-C(6)H_2OH$ group in D-galactose reduces the binding affinity by only 2-fold, but substitution with the apolar $-C(6)H_3$ group in D-fucose lowers affinity by about 40-fold. These affinities are also reflected in the efficiency of active transports of these three sugars. Structures of complexes of ABP with arabinose, galactose and fucose refined at 1.7 Å, 1.8 Å, and 1.9 Å resolutions, respectively, show in atomic details how ordered bound water molecules, coupled with localized changes, can govern substrate specificity and affinity. In all three complexes, the sugar ring is positioned identically in the binding site and each hydroxyl common to these sugars participates in identical hydrogen-bonding interactions. Two ordered water molecules in the site contribute further to tight binding of arabinose but create a much less favorable interaction with the methyl group of fucose. Tight binding of galactose is attained by the replacement of one of the water molecules by its $-C(6)H_2OH$, coordinated with localized structural changes which include a shift and redirection of the hydrogen-bonding interactions of the other water molecules.

Th-AM-SymII-5

THE ROLE OF WATER IN THE PROTEIN FOLDING PROCESS
((M. Sundaralingam and C. Sekharudu)) Department of Chemistry & Ohio State Biotechnology Center, The Ohio State University, Columbus, OH 43210

About 100 unique high resolution (< 1.9Å) x-ray structures of proteins were used to identify intra- and inter-chain water-bridges between the carbonyl and amide groups (cf *M. Sundaralingam and C. Sekharudu, Science, 244 (1989) 1333; and C. Sekharudu and M. Sundaralingam, "Water and Biological Macromolecules", Macmillan Press Ltd, Ed. Eric Westhof, 1992, p148*). The expanded data base has given more information on the hydration of α-helices and also β-sheets and other secondary structures with inserted water molecules. The water-inserted secondary structure-like segments with water molecules bridging the potential secondary structure hydrogen bonding sites viz., $NH_{i+n}...W...CO_i$ are abundant and occur within or adjacent to classical secondary structural elements. Most of these water-bridged segments display conformations that lie between (a) γ-turns and β-turns, (b) β-turns and α-helices, (c) α-helices and π-helices and (d) β-strands and random conformations. Bridging water molecules are frequently found between β-strands at either ends of β-sheets or at the middle where they are invariably associated with bulges. The conformational states of these water-bridged segments and their variability observed in homologous proteins suggests that the peptide segments are probably intermediates in the folding pathway of secondary structures. Water molecules are also found bridging various secondary structural elements in protein tertiary structure. Our analysis suggests a mechanism for the supportive role of water in aiding protein folding as determined by the primary sequence. Energetic considerations for the involvement of water in the folding process will also be presented.

MUSCLE STRUCTURE

Th-AM-E1

TROPONIN-C REMAINS EXTENDED IN THE TERNARY TROPONIN COMPLEX.
((B.-J. Gong, Z. Wang, T. Tao and J. Gergely)) Muscle Research Group, Boston Biomedical Res. Inst., 20 Staniford St., Boston, MA 02114

We have used resonance energy transfer measurements to study the relative disposition of the N- and C-terminal domains of troponin-C (TnC) in the ternary troponin (Tn) complex. By site-directed mutagenesis we produced rabbit skeletal TnC mutants containing two Cys residues, one in each of the N- and C-terminal domains. We used 1,5-IAEDANS as the donor and DDP-Mal as the acceptor attached to the following pairs of residues: 57-98, 49-125, and 12-153. Upon binding of TnI+TnT, in the absence of Ca^{2+} the distance in these pairs does not change, but in the presence of Ca^{2+} it decreases by ~7Å for the 57-98 pair. No significant Ca^{2+}-effect was found for the other pairs. For the free TnC mutants the distances agreed well with those derived from X-ray diffraction (see Strynadka & James, Curr. Opinions in Struct. Biol. *1*, 905, 1991). In comparison, the distance between sites in calmodulin corresponding to the 57-98 pair decreases by 12Å upon binding of a target peptide, and an even larger decrease, ~30Å, takes place for the distance corresponding to the 49-125 pair (Ikura et al., Science *256*, 632, 1992; Meador et al., Science *257*, 1251, 1992). Our results indicate that TnC retains its extended conformation in the ternary Tn complex, as suggested by Blechner et al. (Biochemistry *31*, 11326, 1992) based on low angle X-ray diffraction studies on the complex between TnC and the TnI inhibitory peptide. However, it is apparent that some structural rearrangement does occur in TnC upon binding of TnI+TnT, as reflected by the decrease in distance between residues 57 and 98 (cf. Wang et al, J.B.C. *262*, 9638 1987). These findings will be discussed in light of the regulatory light chain conformation in myosin subfragment-1. (Rayment et al., Science *261*, 50, 1993). (Supported by NIH AR21673 and HL05949, and MDA).

Th-AM-E2

PROXIMITY OF THE MYOSIN REGULATORY LIGHT CHAIN TO THE HEAD-ROD JUNCTION STUDIED USING FLUORESCENCE SPECTROSCOPY
((M. Kekic[1], W. Huang[2], B. Hambly[2] and C.G. dos Remedios[1])) [1]Muscle Research Unit, Anatomy Dept. and [2]Pathology Dept., Sydney University, NSW 2006 Australia.

Fluorescence resonance energy transfer (FRET) spectroscopy was used to measure the distance between a fluorescent probe bound to the S2 region of the myosin heavy chain, close to the head-rod junction, and a probe bound to its regulatory light chain (LC2). We calculated the distance between these two fluorophores to be less than 30Å. The donor probe was bound to a Lys residue located within the S1-S2 link region of the pig cardiac myosin heavy chain, that can be specifically modified with the fluorescent probe 2-(*N*-methylanalino)naphthalene-6-sulphonic acid (MANS) (Hiratsuka, 1981, *J. Biol. Chem.* 256:10645). Approximately 0.9-1.2 moles of MANS probe was bound per mole of myosin. 5-iodoacetamide fluorescein (IAF) was bound to the single Cys residue (Cys 109) of isolated chicken gizzard regulatory light chain. IAF-LC2 was then exchanged onto purified pig cardiac myosin using a method described previously (Hambly *et al.*, 1991, *Biophys. J.* 59:127), achieving 30-50% exchange. After correcting for extent of labelling and exchange, IAF was found to quench MANS fluorescence by greater than 90%, yielding a distance between the probes of approximately 30Å. These results will be discussed in relation to the role of LC2 in modulating the flexibility of the head-rod junction. Supported by the NHMRC of Australia.

Th-AM-E3

OBLIQUE SECTION 3-D RECONSTRUCTION OF RELAXED INSECT FLIGHT MUSCLE REVEALS CROSS BRIDGE LATTICE IN HELICAL REGISTRATION. ((Holger Schmitz, Carmen Lucaveche, Michael K. Reedy and Kenneth A. Taylor)) Department of Cell Biology, Duke University Medical Center, Durham, NC 27710 (Spon. by M. A. Titus)

Independent studies by J. Squire, using M-band filament profiles, and G. Beinbrech, using subfilament orientations in thick filament backbones, suggested that the thick filaments are azimuthally disordered in insect flight muscle. We have computed oblique section 3-D reconstructions from single images of transverse sections of tannic acid-uranyl acetate (TAURAC) fixed, relaxed *Lethocerus* flight muscle. The reconstructions reveal a very regular right-handed helical arrangement of a square profile for the averaged myosin filaments in cross section view. The observed features in an averaged reconstruction encompassing nearly an entire myofibril indicate that the crossbridges even in relaxed muscle are in excellent helical register in the A-band. TAURAC fixation also traps a near complete 38.7 nm labeling of the thin filaments in relaxed muscle marking the left handed helix of actin targets surrounding the thick filaments. However, these crossbridges are much thinner and less massive than those observed in rigor muscle. The regular labeling of the actin targets as well as the regular orientation of the crossbridges would suggest that the thick filament azimuth in the muscle is selected to optimize the alignment of the crossbridges with actin targets. This alignment of 4-fold myosin filament symmetry with the 6-fold screw symmetry of the target lattice will produce rotational disorder in the 6-fold symmetric filament backbones. This hypothesis would thus explain how a regular arrangement of crossbridges could coexist with an apparently random orientation of the subfilament backbones or M-band filament profiles. Supported by NIH.

Th-AM-E4

AN ATOMIC MODEL OF THE UNREGULATED THIN FILAMENT OBTAINED BY X-RAY FIBER DIFFRACTION ON ORIENTED ACTIN-TROPOMYOSIN GELS. ((M. Lorenz, D. Popp, K. Poole, G. Rosenbaum* and K.C. Holmes)) Max-Planck Institut for Med. Research, Heidelberg, Germany, *Biostructures Institute, Philadelphia, PA 19104-3358. (Spon. by K.C. Holmes)

An EM-reconstruction of the thin filament in the on-state by Milligan and Flicker (1987), *J. Cell. Biol.*, 105. shows tropomyosin at an azimuthal position close to the cleft of the actin helix with a binding radius of about 39Å. Based upon X-ray fiber diffraction patterns from oriented actin-tropomyosin gels at a resolution of 8Å we modelled the position of tropomyosin on actin. For the calculations we used the atomic f-actin model by Lorenz *et al.* (1993), *J. Mol. Biol.*, 234, which has been refined against fiber diffraction data by using a Monte-Carlo related method. The atomic structure of tropomyosin was modelled based upon the crystal structure determined by Phillips *et al.* (1986), *J. Mol. Biol.*, 75. The first eight amino acids were removed since they belong to the overlapping region of two tropomyosin strands. The repeat of the coiled coil was set to 128Å to embed tropomyosin in the actin symmetry. Thus, one tropomyosin strand runs exactly along seven actin monomers. The resulting atomic model shows strong electrostatic interactions between charged side chains of tropomyosin residues and actin residues in the helix from Ile309 to Leu320 and the neighboring β-sheet from Lys328 to Ala331 which are located in subdomain 3. The resulting binding radius of 38.5Å and the determined azimuthal position of tropomyosin are in good agreement with the results by Milligan and Flicker (1987). Furthermore, the calculated position allows undisturbed binding of the myosin crossbridges to the suggested actin binding site (Rayment *et al.*, 1993, *Science*, 261).

Th-AM-E5

THE EFFECT OF CALCIUM ON THE REGULATED THIN FILAMENT STRUCTURE ((K.J.V. Poole, M. Lorenz, G. Evans*, G. Rosenbaum+ & K.C. Holmes)) Max Planck Inst. Med. Research, Heidelberg, Germany; * EMBL, DESY, Hamburg, Germany; + Biostructures Institute, Philadelphia, USA.

Obtaining clear X-ray diffraction data from the fully regulated thin filament has proved difficult in oriented gels and overstretched, living muscle fibres. We have used skinned rabbit psoas fibres stretched well beyond overlap to 4.5μm in which the helical diffraction from the myosin head arrangement can be disordered by the removal of ATP. Calcium ions are introduced in the absence of ATP so cross-bridge binding effects are avoided. Using the 0.2 x 0.4mm focus from the mirror/monochromator camera X9B at the NSLS, Brookhaven National Laboratory, camera lengths of 40 and 95cm and the Fuji imaging plate detector we obtained diffraction patterns from the same specimen at different calcium concentrations. The major intensity changes occur on the 1st and 2nd layer lines as observed previously in gel and fibre studies (Popp & Maeda, JMB 229, 279, 1993; Yagi & Matsubara, JMB 208, 359, 1989), and we have carefully quantified these and other smaller changes on the equator and the 6th layer line. Using an atomic model of the actin/tropomyosin filament (Lorenz et. al.- in preparation) based on Holmes et.al., Nature 347, 1990 & Lorenz et. al., JMB, 234, 1993, we show that the data can only be accounted for by a large (ca. 25°) azimuthal rotation of the tropomyosin strand around the actin filament from an off-state position which covers a number of known myosin binding residues. This location would sterically block strong cross-bridge attachment. Interestingly, the titration of the structural change against calcium ion concentration shows that the transition occcurs at a higher calcium concentration and is sharper than the force dependence of this muscle on calcium.

Th-AM-E6

ANIMATED VISUALIZATION OF CROSS-BRIDGE MOTION DURING THE ACTIVE CYCLE ((T.P. Burghardt, and K. Ajtai)) Department of Biochemistry, Mayo Foundation, Rochester, MN 55905.

The angular distribution of myosin cross-bridges in muscle fibers was investigated in four physiological states using a multiple probe analysis of varied extrinsic probes of the cross-bridge. The analysis combines data of complementary techniques from different probes giving the highest possible angular resolution of the gross orientation changes of the myosin head. Spin and fluorescent extrinsic probes of the fast reactive sulfhydryl on myosin subfragment 1 were employed. The combination of the EPR and fluorescence polarization data determined a highly resolved cross-bridge angular distribution in rigor, in the presence of MgADP, in isometric contraction, and in relaxation at low ionic strength. These findings confirm earlier observations of a rigid body rotation of the SH1 region in the myosin head group upon physiological state changes, and, indicate the path and extent of cross-bridge rotation during contraction. An animation of myosin movements in the active cycle is presented with precise 3-D visualization of the polar and torsional motions of the head relative to actin. This work was supported by the NIH (R01 AR 39288), the AHA (GIA 930 06610), and the Mayo Foundation.

Th-AM-E7

LYSINE METHYLATION AND THE ATP SITE OF MYOSIN S-1. D.B.Bivin, K.Ue, M.Khoroshev & M.F.Morales, U.Pacific, 2155 Webster St., San Francisco, CA, 94115.

For some time (e.g., Rainford, et al., Biochemistry 3:1213,1964) it has been thought that various modifications which accelerate the CaATPase of myosin do so by facilitating the escape of the ADP product. A spinoff from Rayment's successful crystallization and structural study of myosin S-1 is (White, Rayment, Biochemistry, 32:9859,1993) that the lysine modification required for crystallization causes such an acceleration (Fig.A). The Ando, et al. (BBRC 109:1,1982) observation that the ATP-binding pocket of S-1 protects e-nucleotides from fluorescence quenching by acrylamide offers a simple test of the pocket condition before and after modification. We have titrated the ATP-binding pocket of S-1 using e-ADP. After lysine-modification according to Wojciech, et al. (Biochemistry, 32:9851,1993) the pocket appears to offer less protection from quenching. This result may bear on contraction hypotheses that assign a transductive role to ATP cleft operation (Rayment, et al., Science, 261:59,1993). Research supported by HL-44200, DMB-900-3692, and a Fogarty Scholarship to M.F.M.)

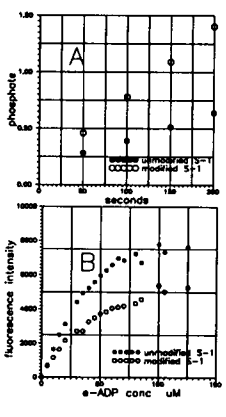

Th-AM-E8

STUDIES OF THE SOLVENT ACCESSIBILITY OF FLUORESCENT NUCLEOTIDES BOUND TO MYOSIN AND TO ACTOMYOSIN. ((Kathleen Franks-Skiba, Thomas Hwang and Roger Cooke)) Dept. of Biochem/Biophysics, and CVRI, UCSF.

We measured the accessibility of ethenoADP (εADP) bound to myosin and εATP during steady state hydrolysis by measuring the quenching of their fluorescence using the solvent phase quencher acrylamide, 25->100mM. Previous investigators have shown that both εATP and εADP are partially buried in the structure of the myosin molecule when bound (Ando et al BBRC, '82). The solvent accessibility of both εADP and εATP, during steady state hydrolysis, varied with both temperature and ionic strength. The nucleotides became more accessible at higher temperatures and higher ionic strength. This result suggests that the nucleotide pocket of myosin can exist in both a closed form that allows little quenching and a more open form that allows some quenching, in agreement with the conclusions reached by Rosenfeld & Taylor (JBC, '84) from studies at a single temperature. At temperatures and ionic strengths close to physiological the more open form would be energetically favored. These results show that the transition between forms is not strongly coupled to the state of the nucleotide nor is it accompanied by large changes in free energy. Although εADP binds only weakly to acto.S1, as determined by sedimentation, the fluorescent component due to specifically bound nucleotide could be determined by a combination of sedimentation and fluorescence in the presence and absence of 5mM ADP. Our preliminary results suggest that the solvent availibility of εADP is higher in Actin•Myosin•εADP than in Myosin•εADP. This result supports the hypothesis of Rayment et al, (Science '93) that the nucleotide pocket opens when myosin binds to actin. Supported by AR30868.

Th-AM-F1

HYDRODYNAMIC INTERACTIONS IN BIOLOGICAL MEMBRANES.
((Daniel A. Hammer, Stuart J. Bussell, Travis Dodd, Donald L. Koch, and Ashok Sangani*)) School of Chemical Engineering, Cornell University, Ithaca, NY 14853 and *Department of Chemical Engineering and Material Science, Syracuse University, Syracuse, NY 13244.

We have calculated how hydrodynamic interactions among membrane proteins affect protein diffusivity in biological membranes. We employ the Saffman model to idealize a membrane as a thin viscous lipid fluid surrounded by lower viscosity aqueous compartments. Membrane proteins are modeled as embedded disks. We solved the Stokes equations for lipid flow between two freely mobile proteins at all protein separations. The hydrodynamic coupling of protein motion is long range, with a length-scale $O(10^3 a)$, where a is the protein radius. Next, we calculated the short time diffusivity at low protein area fraction, ϕ, by non-divergent summation of pairwise hydrodynamic interactions. We found the short time diffusivity $D_S^o = 1 - 1.38\phi$ for typical protein size, membrane thickness, and ratio of viscosities of lipid and aqueous solutions. We are extending our calculations for the short time diffusivity to higher area fractions by numerical solution of Stokes equations for lipid flow using multipole expansion and including lubrication for near-particle approach.

The long-time self diffusivity, D_S^∞, can be obtained by multiplying the short time diffusivity by the dimensionless diffusivity obtained from Monte-Carlo simulations of protein diffusion which include thermodynamic interactions. The combination of hydrodynamic and thermodynamic interactions quantitatively explains experimentally observed reduction in D_S^∞ with increasing ϕ both in cases where all proteins are free to diffuse, and where some fraction of proteins is immobile. Our calculations suggest hydrodynamic interactions may be important determinants of protein diffusivity in membranes.

Th-AM-F2

MOLECULAR DYNAMICS SIMULATIONS OF LIPID:PROTEIN INTERACTIONS: GRAMICIDIN A IN A DMPC BILAYER
((T. B. Woolf and B. Roux)) GRTM & Dept of Chem, Univ of Montreal, Montreal, Canada H3C 3J7

Molecular dynamics methods can provide significant insight into the details of lipid:protein interactions. The proper application of the method requires realistic starting conformations, reasonable estimates for the cross sectional area contributions of protein and lipid, and an empirical potential function which carefully balances the hydrophobic and hydrophilic forces. Gramicidin represents an ideal system for exploring lipid:protein interactions due to the wealth of experimental information available for direct comparison with simulation results. We present the analysis of 300 model systems built for exploring the range of possible beginning points (*Biophys J*, 64, A354) and of five extensive trajectories. Each system represents 8:1 DMPC:gramicidin concentration with 50% weight water as studied by NMR in the laboratories of T. Cross, B. Cornell, and J. Davis. One of the trajectories is for 600 psec, while the other four are for 300 psec each. Equilibration was for 100 psec in all five trajectories. The role of the Trp in interfacial behavior is directly explored through analysis of the hydrogen bonding observed between Trp and water and between Trp and DMPC. Also, attractive VDW interactions between the alkane chains and Trp residues are observed. Overall, the most energetically negative interactions between gramicidin and DMPC lipids are evenly split between electrostatic and VDW terms. This implies a degree of interaction between the lipid head groups and protein and between the lipid alkane chains and protein. A slight ordering of the alkane chains by gramicidin at this concentration was observed. Density profiles of the atomic distribution averaged over the full trajectory are presented. The results suggest that this method can offer considerable insights into details of protein:lipid interactions that would not be possible from direct experiment.

Th-AM-F3

CALORIMETRIC DETECTION OF CURVATURE STRAIN IN PHOSPHOLIPID BILAYERS.
((R.M. Epand and R.F. Epand)) McMaster University, Hamilton, Ontario L8N 3Z5.

Certain phospholipids, when constrained to pack into planar bilayers, will form unstable structures as a consequence of their molecular shape and non-covalent bonding. This produces curvature strain which may provide energy for certain membrane processes. We demonstrate that an exothermic process associated with the relief of curvature strain can be detected calorimetrically. The enthalpy of incorporation of lysophosphatidylcholine (LPC) into large unilamellar vesicles of monomethyldioleoylphosphatidylethanolamine (MeDOPE) at pH 7.4 is exothermic but it is endothermic for stable bilayers such as this same lipid at pH 9 or dioleoylphosphatidylcholine at pH 7.4 or 9. The addition of LPC to MeDOPE at pH 7.4 is exothermic only for the addition of the first few percent of LPC and then it becomes endothermic. The size of the exothermic heat change is sensitive to changes temperature, while the endothermic processes are relatively temperature insensitive. The exothermic heat is also larger when 1 or 2 mol % of diolein is incorporated in the vesicles of MeDOPE. These results are all consistent with the exothermic process corresponding to the relief of curvature strain in bilayers having a tendency to convert to the hexagonal phase. It provides a demonstration that considerable energy may be released upon the incorporation of certain molecules into membranes which have a low radius of spontaneous curvature.

Th-AM-F4

APPLICATION OF SMALL ANGLE NEUTRON SCATTERING TO DETERMINE PROPERTIES OF THE MEMBRANE-WATER INTERFACE.
((R.M. Epand, B.D. Gaulin, J. Avelar and C. Brodie)) McMaster University, Hamilton, Ontario L8N 3Z5.

Most x-ray and neutron diffraction studies of membranes have focused on the Bragg reflections to determine the symmetry elements and dimensions of the periodic structures present in these samples. However, there is additional information present in the small angle scattering peak which is sensitive to the nature of the membrane-water interface. The properties of this interface likely modulate a number of membrane dependent phenomenon such as membrane fusion and the activity of membrane bound enzymes. We have measured and analyzed the small angle neutron scattering (SANS) from multilamellar vesicles of dipalmitoylphosphatidylcholine (DPPC) and 1-palmitoyl-2-oleoylphosphatidylethanolamine (POPE) in buffer made with ^2H_2O. We have fit the SANS to a sum of Guinier, Porod and Bragg scattering terms. We observe that the SANS intensity increases markedly when DPPC is in the P_β' phase. This is in accord with the increased surface area expected for this ripple phase. In addition, the Porod scattering term for POPE exhibits a marked decrease in intensity as the temperature is increased through the L_β to L_α phase boundary. This change is in the direction expected for the interface becoming more diffuse as the bilayer undergoes melting. The results suggest that SANS may provide a novel method to ascertain the texture of the membrane interface.

Th-AM-F5

INTERNUCLEAR DISTANCE MEASUREMENTS IN MEMBRANES USING ROTATIONAL RESONANCE NMR.
((Steven O. Smith)) Department of Molecular Biophysics and Biochemistry, Yale University, New Haven, CT 06511.

Rotational resonance (RR) NMR methods are explored for determining intramolecular and intermolecular distances between ^{13}C-labeled sites in membrane bilayers. Specific ^{13}C-labels have been incorporated into peptides corresponding to the transmembrane (TM) domain of glycophorin A to examine the local secondary structure and tertiary interactions in a membrane environment. Magnetization exchange rates measured between V_{80} [1-^{13}C] and G_{83} [2-^{13}C] and between M_{81} [1-^{13}C] and G_{83} [2-^{13}C] in the middle of the transmembrane sequence correspond to internuclear distances of ~4.5 Å, consistent with a helical peptide structure. Longer distances are observed between I_{95} [1-^{13}C] and G_{98} [2-^{13}C] which argue that the transmembrane helix unravels at the membrane interface. Intermolecular magnetization exchange measurements between several ^{13}C sidechain methyl labels and backbone carbonyl labels indicate that V_{80} and V_{84} are in the dimer interface. Specific ^{13}C labels have also been incorporated into DPPC. Intramolecular magnetization exchange rates measured between the 1-position of the *sn*-1 acyl chain (1-[1-^{13}C]) and 2-position of the *sn*-2 acyl chain (2-[2-^{13}C]) of DPPC correspond to distances of ~4.5 to 5.0 Å. These results are consistent with a smaller axial displacement (1.0-2.0 Å) between the *sn*-1 and *sn*-2 acyl chains than observed in the crystal structure of DMPC (~3.6 Å). In addition, intermolecular magnetization exchange rates have been measured between 1,2-[2-^{13}C] DPPC and the ^{13}C-OH position of Y_{93} in the glycophorin TM peptide. These intermolecular distance measurements demonstrate that the relative orientation and location of membrane lipids and peptides can be established using RR NMR methods.

Th-AM-F6

DYNAMICS OF PHOSPHOLIPID MEMBRANES STUDIED BY DEUTERIUM NMR RELAXATION.
((Michael F. Brown, Theodore P. Trouard, Constantin Job, and Todd M. Alam)) Department of Chemistry, University of Arizona, Tucson, Arizona 85721.

An understanding of the **biophysical properties** of membrane constituents is vitally important with regard to knowledge of their mechanisms of action. Local segmental motions of the lipids may be involved in rapid transmembrane movement of non-polar solutes; molecular motions due to lateral diffusion of lipids and proteins may govern formation of transient enzyme complexes; equilibrium and dynamical properties of the bilayer may influence lipid-protein interactions linked to key biological functions; and collective undulatory excitations[1] may yield repulsive forces implicated in membrane fusion. In deuterium (^2H) NMR spectroscopy, the motionally averaged lineshapes give knowledge of **equilibrium properties**, whereas the corresponding relaxation rates reflect **dynamical properties**. Using ^2H NMR relaxation methods we have tested the hypothesis that the dynamics of membranes involve **relatively slow collective excitations** of the molecular assembly of phospholipids. The small contribution from local internal motions suggests that the microviscosity corresponds to essentially liquid hydrocarbon[2] in agreement with **molecular dynamics simulations** of membrane bilayers.[3] This talk will describe briefly the experimental and theoretical basis for these conclusions. [1]M.F. Brown (1982) *J. Chem. Phys.* 77, 1576-1599. [2]M.F. Brown et al. (1983) *PNAS* 80, 4325-4329. [3]R.M. Venable et al. (1993) *Science* 262, 223-226. Supported by NIH grants GM41413 and EY03754.

Th-AM-F7

KINETICS OF SURFACE CHANGES OF LARGE UNILAMELLAR VESICLES INDUCED BY OSMOTIC SHRINKAGE.
((E.A. Disalvo, A.M. Campos,E.Abuin, H.Chaimovich and E.A. Lissi)) Universidad de Buenos Aires, Argentina, Universidad de Sao Paulo, Brasil and Universidad de Santiago de Chile, Chile.

The shrinkage of large unilamellar vesicles (LUV's) of dipalmitoylphosphatidylcholine in the liquid crystalline state promotes an upward shift of the surface potential as measured with fluorescent probes. The rate of the changes in the surface correlates with an increase in the optical density of the dispersion and it is several times faster than the water outflux provoked by the osmotic gradient. At equilibrium, shrunken vesicles show an increased polarization of the surface in the head group region with little and none effects on the hydrocarbon region near the head groups and the hydrocarbon core respectively. The osmotic collapse does not change the transition temperature although affects the surface properties of the gel and the fluid state. It is interpreted that LUV's volume decreases in a first stage with a change in the corrugation of the bilayer. The second stage of water outflux would promote a volume decrease maintaining the same total area.(With funds from: FUNDACION ANTORCHAS-ANDES; TWAS;UBA and CONICET (Argentina)

Th-AM-F8

PERTURBATION OF BILAYER MEMBRANE STRUCTURES BY THE HYDROPHOBIC MOLECULE SQUALENE.
((K. Lohner*, G. Degovics* and F. Paltauf+)) *Institute of Biophysics and X-Ray Structure Research, Austrian Academy of Sciences and +Department of Biochemistry, Technical University of Graz, A-8010 Graz, Austria. (Spon. by. Shyamsunder Erramilli).

An X-ray diffraction study on the lipid-polymorphism of aqueous dispersions of mixtures between synthetic 1-stearoyl-2-oleoyl-phosphatidylethanolamine (SOPE) and 1-palmitoyl-2-oleoyl-phosphatidylcholine (POPC) in the presence of squalene, an intermediate in the biosynthesis of sterols, has been performed. Cellular concentrations of this molecule are usually low, but for example large quantities accumulate in fungi treated with specific inhibitors of squalene epoxidase. Testing whether squalene, owing to its hydrophobic character, might disturb the bilayer structure of membranes and thus might effect membrane-associated processes was an incentive to this study.

In fact, the bilayer stabilizing effect of POPC, as indicated by shifting the lamellar to inverse hexagonal phase transition of the lipid mixtures to higher temperatures with increasing concentrations of POPC, was reversed by adding squalene. Furthermore, under certain experimental conditions, e. g. SOPE/POPC (95/5 mol/mol) and 6 Mol% squalene, this transformation was even overlapping with the lamellar gel to fluid phase transition. An unrefined phase diagram of SOPE as a function of added POPC and squalene, defining the stability range of the lamellar and non-lamellar phases, as well as the limiting partition of squalene into the membrane will be presented.

Th-AM-F9

MONOLAYERS OF VECTORIALLY ORIENTED PHOTOSYNTHETIC REACTION CENTERS TETHERED TO THE SURFACE OF INORGANIC SUBSTRATES.
((J.A. Chupa, J.P. McCauley, Jr., R.M. Strongin, A.B. Smith, III, J.K. Blasie*; L.J. Peticolas and J.C. Bean**)) *Department of Chemistry, University of Pennsylvania, Philadelphia, PA 19104 and ** AT&T Bell Laboratories, Murray Hill, NJ 07974. (Spon. by J.K. Blasie)

We have demonstrated that a single monolayer of the photosynthetic reaction center integral membrane protein, can be selectively and reversibly tethered to the surface of an inorganic substrate. A bifunctional, organic self-assembled monolayer (SAM), chemisorbed to the inorganic substrate and possessing amine surface endgroups, electrostatically tethered the reaction centers, forming a single monolayer of vectorially oriented molecules with approximately close-packed in-plane densities. Definitive structural results were obtained utilizing Ge/Si multilayer substrates, fabricated by molecular beam epitaxy, which enabled us to use x-ray interferometry to derive the profile structures of the composite multilayer substrate-SAM/reaction center system to ~7 Å resolution and prove its correctness via x-ray holography. Optical absorption measurements performed on the tethered protein monolayer system were consistent with the x-ray diffraction results indicating the reversible formation of a densely packed single monolayer of fully-functional reaction centers on the surface of the SAM. The importance of utilizing the organic self-assembled monolayer lies in its ability to specifically tether detergent-solubilized integral membrane proteins to produce novel model membrane systems.

Th-AM-F10

ANOMALEOUS SWELLING OF LIPID BILAYERS

Thomas Hønger,[a] Kell Mortensen,[b] John Hjort Ipsen,[a] Jesper Lemmich,[a] Rogert Bauer,[c] and Ole G. Mouritsen,[a]

[a]Department of Physical Chemistry, The Technical University of Denmark, Building 206, DK-2800 Lyngby, Denmark
[b]Department of Solid State Physics, Risø National Laboratory, DK-4000 Roskilde, Denmark
[c]Department of Physics, Royal Danish School of Agricultural and Veterinary Sciences, Thorvaldsensvej 40, DK-1871 Frederiksberg, Denmark

Small-angle neutron scattering is used to determine the temperature dependence of the lamellar repeat distance in an aqueous multilamellar solution of phospholipid bilayers. A dramatic thermal anomaly in the swelling behavior is observed at the bilayer phase transition. The anomalous behavior can be suppressed by varying the acyl-chain length or by alloying with a molecular stiffening agent, such as gramicidin. The experimental results are explained in terms of renormalization of the bilayer curvature elasticity using a theory of repulsive interlamellar undulation forces.

LIGAND-GATED CHANNELS

Th-AM-G1

CLONING OF A cDNA FOR THE HIGH AFFINITY SULFONYLUREA RECEPTOR FROM PANCREATIC α- and β-CELLS. ((J. Bryan, L. Aguilar-Bryan and D.A. Nelson)) Depts of Cell Biology and Medicine, Baylor College of Medicine, Houston, TX. (Spon. by J. Bryan)

We have used a radioiodinated derivative of the antidiabetic sulfonylurea, glyburide, to photolabel the pancreatic α- and β-cell high affinity sulfonylurea receptor. The 140 kDa radioiodinated receptor has been purified ~2500-fold from hamster insulin secreting tumor (HIT) cells using ConA-agarose, Reactive Green 19-agarose, phenylboronate 10-agarose and SDS gel electrophoresis. The purified protein has been digested with V8 protease and used to obtain N-terminal amino acid sequence. Antipeptide antibodies generated using this peptide sequence precipitate the 140 kDa radioiodinated receptors from all three rodents and can be displaced by the immunizing peptide, but not by unrelated peptides. Degenerate oligonucleotides based on the N-terminal sequence were used in a PCR strategy to clone a cDNA fragment from a randomly primed mouse α-cell (αTC-6) cDNA library. This cDNA encoded all 28 amino acids corresponding to the sequence obtained by chemical methods and was used to screen HIT, rat (RIN) β-cell and mouse α-cell libraries. Partial sequencing of these cDNAs indicates the receptor is very similar between these species, has multiple membrane spanning domains as defined by hydrophobicity analysis and has at least one, and probably two, potential ATP binding sites. Preliminary data put the N-terminus of the mature receptor on the outside of the membrane with a glycosylated *asn* residue within the first ten amino acids and suggest the receptor is inserted into the membrane via a signal peptide. We are using the RIN cDNA clone to transcribe mRNA *in vitro* for injection into oocytes to determine if the receptor has ATP-sensitive K^+ channel activity and to construct eukaryotic expression vectors to demonstrate high affinity sulfonylurea binding.

Th-AM-G2

NICOTINIC RECEPTOR LIGAND-BINDING DOMAIN PROBED BY CYSTEINE-SUBSTITUTION MUTAGENESIS. ((James McLaughlin, Edward Hawrot*, and Gary Yellen)) Dept. of Neurobiology, Harvard Medical School and Mass. General Hospital, Boston, MA 02115; *Molecular and Biochemical Pharmacology, Brown University, Providence, RI 02912.

We constructed a series of mouse muscle nicotinic receptor mutants that have a cysteine substituted for one of the amino acid residues in the alpha subunit between positions 181 and 198. Properties of the mutants were examined by co-expression with the β, γ and δ subunits in *Xenopus* oocytes. Two-electrode voltage clamp was used to compare the responses to acetylcholine of cysteine-containing mutants with those of the wild type receptor. Many of these mutant receptors give responses to ACh comparable to wild type in both magnitude and EC_{50}. Mutants were also assessed by ^{125}I-α-bungarotoxin binding; association and dissociation kinetics of binding were similar to those of the wild type.

The effect of sulfhydryl-specific modifying reagents on ACh-evoked currents was examined using methyl methanethiosulfonate (MMTS). Several mutants, particularly αV188C and αH186C, showed significant decreases in response to ACh following modification by MMTS; these effects were at least partially reversed by dithiothreitol. We also examined the effect of MMTS and several other reagents on α-bungarotoxin binding. One of these, 4-(chloromercuri) benzenesulfonic acid (PCMBS) significantly decreased the α-bungarotoxin B_{max} to αV188C and αH186C without altering binding kinetics.

Th-AM-G3

HYBRID CHANNELS FORMED FROM CO-ASSEMBLY OF RETINAL ROD AND OLFACTORY CYCLIC NUCLEOTIDE-GATED CHANNEL PROTEINS.((J.T. Finn, J.E. Schroeder, T.-Y. Chen and K.-W. Yau)) Howard Hughes Med. Inst. and Dept. of Neurosci., Johns Hopkins School of Medicine, Baltimore, MD 21205. (Spon. by S. Kuo)

Cyclic nucleotide-gated cation channels play a central role in visual and olfactory transductions. In addition, there is now evidence that homologous channels also exist in other tissues. The question remains whether the subunits forming these channels belong to different subfamilies (as with the *Drosophila* potassium channels) or whether they are all members of a single family that can co-assemble in different combinations to give a variety of channels with different properties. We addressed this question by examining whether the cloned rod photoreceptor and olfactory channel proteins can form hybrid channels. We expressed cDNAs encoding the human rod channel (subunit 1) and the rat olfactory channel in HEK 293 cells and studied cyclic nucleotide-gated channel activity in excised, inside-out patches. The homomeric rod and olfactory channels bind cGMP with $K_{1/2}$ values of 60-80 μM and 1-3 μM, respectively. Patches from cells co-transfected with both cDNAs gave a spectrum of $K_{1/2}$ values intermediate between these values, and the shape of the dose-response curves cannot be explained by assuming that the patches contained only two populations of homomeric channels. Further evidence for co-assembly came from experiments with the recently cloned subunit 2 of the rod channel. Although this subunit does not form functional channels by itself, it introduces flickery channel kinetics and L-*cis*-diltiazem block when co-expressed with the olfactory channel, as it does with subunit 1 of the rod channel. In conclusion, it appears that at least the rod and olfactory channels can co-assemble.

Th-AM-G4

A NOVEL MODEL FOR VOLTAGE-DEPENDENT BLOCK OF ION CHANNELS

J. Peter Ruppersberg, Eberhardt von Kitzing, Willy Günther, Peter H. Seeburg, Thomas Kuner, Bert Sakmann, Nail Burnashev and Ralf Schoepfer

Block of the cloned NR1/NR2A NMDA receptor channels by external magnesium (Mg^{2+}) was studied in inside-out patches, inside-out giant patches and outside-out patches from *Xenopus* oocytes. Concentration-dependence of single channel conductance was found to have K_D value of only 0.5 mM. If only internal ion concentration was changed the voltage of half-maximal block shifted with the reversal potential. This suggests that NMDA receptor channels are strongly negatively charged. Similar as previously shown for Mg^{2+} also the charged polyamine toxin Argiotoxin636 (ATX) exhibited both external and internal block of NR1/NR2A receptors. Assuming a fourfold charge of ATX the electrical distances were almost 100% from both sides of the channel. ATX block from both sides of the channel was even increased if instead of NR1/NR2A receptors NR1(S599N)/NR2A(N596S) receptors were used which were not blocked by Mg^{2+} but have an increased Mg^{2+} permeability indicating that the toxin may reach the same blocking site from both sides of the channel. Mg^{2+} block was also dependent on the monovalent ion species. This dependence of voltage of half maximal block and electrical distance was independent of the respective reversal potential suggesting a direct interaction between Mg^{2+} and other ions in the channel. A model which may theoretically explain excessive voltage-dependence and interaction of monovalent ions with the blocking ion in terms of an ion-ion interaction value is presented.

Max-Planck-Institut für medizinische Forschung, Abteilung Zellphysiologie, and Center for Molecular Biology, University of Heidelberg, 69028 Heidelberg, Germany

Th-AM-G5

CLONING AND FUNCTIONAL EXPRESSION OF A PUTATIVE SECOND SUBUNIT OF THE OLFACTORY CYCLIC NUCLEOTIDE-GATED CHANNEL. ((E.R. Liman and L.B. Buck)) Dept. Neurobiology, Harvard Medical School, Boston Ma 02115.

Signal transduction in olfactory neurons occurs through a cascade of events, beginning with the activation of G-protein coupled odorant receptors and resulting in the opening of cyclic nucleotide-gated channels. A cyclic nucleotide- gated channel has been cloned from rat olfactory epithelium (Dhallan et. al, *Nature* 347:184-187, 1990); however, functional differences between this and the native channel suggest the possibility that the native channel is a heteromultimer.

We have cloned a putative second subunit of the olfactory cyclic nucleotide gated channel from a rat olfactory epithelium cDNA library. The cDNA (ROC2) encodes a protein of 574 amino acids with 50% identity to the rat olfactory channel (OCNC) in the region of homology and 80% identity in the cyclic nucleotide binding domain. Several interesting features of this protein include a relatively short amino terminus, a highly charged S4 region and several amino acid substitutions in the highly conserved pore region. *In situ* hybridization demonstrates the expression of the ROCN2 channel mRNA in the olfactory epithelium in a distribution similar to that of the OCNC mRNA.

Functional studies are currently being carried out by expression of the ROCN2 channel in Xenopus oocytes. While expression of the OCNC cRNA gives rise to large cyclic nucleotide-gated currents, we were unable to detect any cyclic nucleotide-gated channel activity in oocytes injected with ROCN2 cRNA. However, we find that co-injection of the two cRNAs leads to channel activity that differs both at the single channel and the macroscopic level from that seen in oocytes injected with the OCNC cRNA.

Th-AM-G6

DISSECTING THE ACTIVATION MECHANISM OF RETINAL ROD cGMP-GATED CHANNELS USING COVALENTLY-TETHERED LIGANDS

((R. Lane Brown & Jeffrey W. Karpen)) Department of Physiology, University of Colorado School of Medicine, Denver, CO 80262.

Cyclic nucleotide-gated ion channels are emerging as the target of an increasing number of signaling pathways. In retinal rods the channel is opened by the binding of at least three molecules of cGMP, but the detailed allosteric mechanism of channel activation remains to be worked out. As a new approach to this problem, we have developed a photoaffinity analog of cGMP, 8-*p*-azidophenacylthio-cGMP (APT-cGMP), that will permanently activate channels in excised membrane patches exposed to UV light. As the fraction of permanently-activated channels increased, the remaining inactive, but partially-liganded channels were opened at lower concentrations of cGMP with reduced cooperativity. When > 80% of the channels in a patch have been permanently activated, binomial statistics predicts that the remaining channels should be missing only the final ligand. Dose-response relations measured under these conditions have revealed a previously unknown heterogeneity in the cGMP binding sites. The relations were much shallower than expected for single-site activation, but were fit rather well as the sum of two populations of sites with widely different affinities (apparent K_D's of about 1 and 25 μM). Although the origin of this heterogeneity is unknown, we are testing two intriguing possibilities: the heterogeneity may arise from differences in cGMP-binding affinity between two distinct subunits that are thought to comprise the native channel, or it may be caused by covalent modulation of the channel's binding sites by phosphorylation. The development of a tethered ligand affords the unique opportunity to study the allosteric mechanism of a channel that does not desensitize and is gated by multiple ligands.

Supported by NIH grants EY09275 and EY06425.

Th-AM-G7

THE M_2 PROTEIN OF INFLUENZA A VIRUS FORMS AN ION CHANNEL IN MAMMALIAN CELLS ((C. Wang#, L.J. Holsinger, R.A. Lamb#, and L.H. Pinto*)) Dep't of Biochemistry, Molecular Biology and Cell Biology, #Howard Hughes Medical Institute, and *Dep't of Neurobiology and Physiology, Northwestern Univ., Evanston, IL 60208

Evidence from the oocyte expression system suggested that the small membrane protein M_2 of influenza A virus is an ion channel. Since this channel is thought to play a role in the viral infection of mammalian cells, we tested to see if M_2 indeed forms an ion channel in mammalian cells. We expressed M_2 in CV1 cells by infecting the cells with recombinant SV40 virus. Whole cell patch clamp showed that the cells that expressed wild type M_2 gave currents which were not voltage-activated, as had been observed for the current in oocytes. The current in CV1 cells was activated by low pH and inhibited by 100 µM amantadine hydrochloride (an anti-influenza A drug). An amantadine resistant mutant, M_2 del28-31, gives hyperpolarization-activated currents in oocytes. A current with a similar time course and voltage dependence was also seen in CV1 cells that expressed M_2 del28-31. This current was amantadine-resistant. These results taken together suggest that M_2 is an ion channel in mammalian cells.

Th-AM-G8

THE TRANSMEMBRANE TOPOLOGY OF GOLDFISH KAINATE RECEPTORS. ((Z. Galen Wo and Robert E. Oswald)) Department of Pharmacology, Cornell University, Ithaca, NY 14853 USA. (Spon. by Z. Galen Wo)

Cloning of cDNAs encoding two goldfish kainate receptors has been reported (Wo & Oswald, *Biophys. J.*, **64**: 326, 1993). These include: GFKARα, which encodes a 45 kD polypeptide, and GFKARβ, which encodes a 41 kD polypeptide that binds kainate with high affinity (K_D of approximately 25 nM). Since all four consensus N-glycosylation sites (Asn-X-Ser/Thr) in GFKARα are located in the proposed cytoplasmic loop between the presumed transmembrane domains (TM) III and IV, GFKARα would not be expected to exhibit N-glycosylated. However, the protein is N-glycosylated *in situ* (Ziegra *et al.*, *Mol. Pharm.* 42:203-209, 1992). A rabbit reticulocyte *in vitro* translation/translocation system supplemented with microsomal membrane was used to examine the N-glycosylation of GFKARα and GFKARβ. In this system, GFKARα is indeed N-glycosylated; whereas, as expected, GFKARβ is not. Expression of truncated GFKARα and site-directed mutagenesis showed that Asn 307 of GFKARα is one of the two functional sites. A chimera constructed from the N-terminal half of GFKARβ and the remainder of GFKARα C-terminal half is also N-glycosylated, indicating that GFKARα and GFKARβ have the same transmembrane topology. These results indicate that at least a portion of the segment between the proposed TMIII and TMIV is actually located extracellularly. Furthermore, deletion of the proposed channel forming TMII did not alter the N-glycosylation of GFKARα, suggesting that the proposed TMII may not cross the membrane in the initial translation/translocation steps. Alternative models for the transmembrane topology of kainate receptors are proposed. These models may have some general implications concerning the formation of ligand binding domain, channel pore, and the regulation sites of ionotropic glutamate receptors.

Th-AM-H1

DIFFUSION OF IP_3, BUT NOT Ca^{2+}, IS NECESSARY FOR IP_3-INDUCED Ca^{2+} WAVES ((M. S. Jafri and J. Keizer)) Institute of Theoretical Dynamics, University of California, Davis 95616

Calcium waves in *Xenopus* oocytes and some other cell types result from agonist induced IP_3 release. Because the diffusion constant for Ca^{2+} is much smaller than that of IP_3, it has been suggested recently that diffusion of Ca^{2+} determines the speed of the wave. We have explored this question using simulations with a realistic model of IP_3-induced Ca^{2+} oscillations [DeYoung and Keizer, PNAS 89 9895 (1992)] combined with diffusion of IP_3 and buffered diffusion of Ca^{2+}. Our results indicate that diffusion of Ca^{2+} plays only a minor role in the observed calcium waves. We show that the waves are primarily kinematic in nature, with variable wavelengths and speeds that depend primarily upon the phase differences between oscillators at different spatial points. These phase differences can be set either by an initial pulse of Ca^{2+} or IP_3 and change only very slowly due to the slow rate of Ca^{2+} diffusion. In the case of a pulse of IP_3, the period of the oscillations is set by the rate of production of IP_3, while the wave speed approximately satisfies the relationship speed = wavelength/period. Although the presence of calcium diffusion changes the wave speed, it is not necessary for the apparent wave propagation. Our results suggest a new role for the diffusion of IP_3 in the observed waves, and that "waves" are, in large part, localized cycles of Ca^{2+} uptake and release that are out of phase.

Th-AM-H2

SIGNALLING PROCESSES IN EXOCRINE ACINAR CELLS AFTER CHOLINERGIC AND ADRENERGIC STIMULATIONS.
((S. Dissing, J. Gromada, T. D. Jørgensen, K. Tritsaris and B. Nauntofte)) Dept. Med. Physiol. Panum Institute, University of Copenhagen, Blegdamsvej 3, 2200 N, Denmark.

We have studied the cellular signalling processes causing release of Ca^{2+} from intracellular pools in parotid and lacrimal acinar cells. On cholinergic stimulation of cells in suspension, there is correlation between the increase in the inositol-1,4,5 trisphosphate ($Ins(1,4,5)P_3$) concentration and the rise in $[Ca^{2+}]_i$. From measurements of the rate of $[Ca^{2+}]_i$ rise in single cells applying digital imaging, we then found the rate of the cellular $Ins(1,4,5)P_3$ rise. Assuming a given $Ins(1,4,5)P_3$ diffusion coefficient we calculated the rate by which Ca^{2+} release processes can be induced by $Ins(1,4,5)P_3$. Our data reveal that the $Ins(1,4,5)P_3$ generated at the plasma membrane, can rapidly diffuse into local areas and release Ca^{2+} from the internal pools causing the synchronous Ca^{2+} rise in the cell. In contrast, when acinar cells are stimulated by adrenaline, only little $Ins(1,4,5)P_3$ is synthesized. After specific α-adrenergic stimulation with phenylephrine, inositol phosphate synthesis is completely absent although $[Ca^{2+}]_i$ is raised by 100 nM. Simultanous α- and ß-adrenergic stimulation will enhance the rise in $[Ca^{2+}]_i$ induced by phenylephrine. Consequently, ß-adrenergic stimulation enhances the Ca^{2+} signalling processes induced by the α-adrenergic receptor.

Th-AM-H3

LOSS OF ENDOPLASMIC RETICULUM Ca^{2+}-ATPase ACTIVITY IN DIABETIC MOUSE ISLETS OF LANGERHANS. ((M. W. Roe, C. J. Frangakis, R. J. Mertz, M. E. Lancaster, B. Spencer, J. F. Worley III and I. D. Dukes)). Department of Medicine, University of Chicago, Chicago, IL 60637 and Glaxo Research Institute, Research Triangle Park, NC 27709.

Non-insulin-dependent diabetes mellitus (NIDDM) is associated with abnormal insulin secretion. The pathogenic mechanisms of this disease are unknown. The stimulation of insulin secretion by glucose depends upon an increase in intracellular Ca^{2+} concentration ($[Ca^{2+}]_i$). This increase is triggered by membrane depolarization that causes influx of Ca^{2+} through voltage-dependent Ca^{2+} channels and release of Ca^{2+} from the endoplasmic reticulum (ER). Using fura-2-loaded single islets derived from diabetic C57BL/KsJ (*db/db*) mice, an animal model of NIDDM, we characterized glucose-induced changes in $[Ca^{2+}]_i$. After stimulating with 12 mM glucose, *db/db* islets lacked a thapsigargin-sensitive reduction of $[Ca^{2+}]_i$, and the $[Ca^{2+}]_i$ oscillations found in non-diabetic control (*db/+*) islets were replaced by a sustained steady-state elevation of $[Ca^{2+}]_i$. These effects were correlated with the development of hyperglycemia *in situ*, and were reproduced *in vitro* with *db/+* islets that had been incubated with 30 mM glucose for 7 days. The results implied that glucose-stimulated activation of ER Ca^{2+}-ATPase (SERCA) was inhibited in the *db/db* islets. Biochemical analysis of islet homogenates showed that thapsigargin-sensitive SERCA activity was 3.8 nmole P_i/µg protein/hr in *db/+* islets, whereas in *db/db* islets, no activity was detectible. Our findings suggest that SERCA may be regulated by the extracellular glucose environment, and indicate that abnormalities of ER Ca^{2+} sequestration might be important in mediating the secretory defects connected with NIDDM.

Th-AM-H4

ALTERATION OF INTRACELLULAR Ca^{2+} TRANSIENTS IN CELLS TRANSFECTED WITH THE cDNA ENCODING SKELETAL MUSCLE RYANODINE RECEPTOR CARRYING A MUTATION ASSOCIATED WITH MALIGNANT HYPERTHERMIA.
((F. Larini[1], F. Zorzato[1], P. Menegazzi[1], T.H. Steinberg[2], M. Koval[2], B. Vilsen[3], J. Andersen[3] and S.Treves[1]))[1]Inst. Gen. Path., Univ. of Ferrara, Ferrara, Italy. [2]Wash. Univ. School of Med., St. Louis, Missouri, USA. [3]Dept. Physiol., Aarhus Univ., Aarhus, DK. (Spon. by C. Sorgato)

Malignant hyperthermia (MH) is an inherited neuromuscular disease in which hypermetabolism, a rapid increase in body temperature and skeletal muscle rigidity are triggered by inhalational anaesthetics and muscle relaxants. Calcium release from the sarcoplasmic reticulum ryanodine receptor (RYR) calcium channel appears to be abnormal in MH and an Arg to Cys mutation has been identified in the RYR from some MH families and in the MH-susceptible pig. However no direct evidence has been obtained indicating that this mutation alters RYR-mediated calcium release. We show by single-cell fluorescence ratio imaging , that COS-7 cells transfected with the RYR cDNA carrying the Arg to Cys mutation have abnormal cytosolic calcium transients in response to the RYR agonist.

Th-AM-H5

PULSED-LASER IMAGING OF RAPID Ca^{2+} SIGNALING IN EXCITABLE CELLS. ((Jonathan Monck, Ariel Escobar*, Iain Robinson, Julio Vergara* and Julio Fernandez)) Mayo Clinic, Dept. of Physiol. and Biophys., Rochester, MN 55905 and *Dept. of Physiol., UCLA, Los Angeles, CA 90024

Excitable cells are thought to respond to action potentials by forming short-lived and highly localized Ca^{2+} gradients near sites of Ca^{2+} entry or Ca^{2+} release from intracellular stores. However, conventional imaging techniques lack the spatial and temporal resolution to capture these gradients. Here we demonstrate that a combination of pulsed-laser microscopy and image restoration by deconvolution that allows capture of Ca^{2+} gradients over millisecond timescales. In patch clamped adrenal chromaffin cells, Ca^{2+} gradients develop at discrete (~1 μm^2) submembrane domains, or hotspots, in response to brief (<50ms) depolarizations. Complete rings of elevated Ca^{2+} are seen only for longer depolarizations. These results argue against models where exocytosis is caused by large ring-like Ca^{2+} gradients beneath the cell membrane and suggests that exocytosis may occur at active zone like structures in chromaffin cells. In frog skeletal muscle fibers, action potentials induce large, short lived Ca^{2+} gradients within individual sarcomeres of skeletal muscle. Gradients are first apparent after the (~3ms) triadic delay, reach a peak 2-3 ms later and then dissipate over 5-10 ms. These results confirm the hypothesis that Ca^{2+} release occurs predominantly from the terminal cisternae of the sarcoplasmic reticulum. The ability to image Ca^{2+} with both high spatial and temporal resolution permits, for the first time, the capture and critical examination of rapid Ca^{2+} signaling events such as those underlying excitation-secretion and excitation-contraction coupling. In addition, this approach can be readily modified to capture rare and/or transient events such as fusion pore opening.

Th-AM-H6

PYRIDINE NUCLEOTIDE FLUORESCENCE (PNF) AS AN INDICATOR OF CHANGE IN MITOCHONDRIAL METABOLISM DURING ACTIVATION OF INSULIN SECRETING CELLS.(R.M. Lynch, L.S. Tompkins and G. Parnami), University of Arizona, Tucson AZ 85724. (Sponsor: J.M. Burt).

Pyridine Nucleotides (PN) are metabolic cofactors that fluoresce at 450 nm when excited by light near 340 nm. PNF has been used as an indicator of metabolic changes in a variety of cell types, however, the exact origin of the PNF under specific experimental conditions is arguable. In the present work we have analyzed the subcellular distribution of PNF in insulin secreting HIT-T15 and isolated beta cells grown in culture. Areas of high PNF co-localize with mitochondria. In addition, glucose and glutamine induced changes in PNF originate primarily from mitochondria as determined by 3D imaging of PNF and a mitochondrial specific dye tetramethyl-rhodamine, methyl ester (TMRE) from single cells. The time course of change in PN fluorescence and intracellular Ca++ were studied in single HIT-T15 cells using spectroscopic imaging to simultan- eously monitor the fluorescence intensity of Calcium Green and NADH. A variable time course in response to substrates was observed among individual cells. In addition, a significant number of cells do not respond. However, in all cases elevations in intracellular Ca++ followed substrate induced increases in mitochondrial PNF. These findings are consistent with previous studies performed in unitary beta cells (EMBO J. 9:53, 1990) indicating mitochondrial metabolism of substrates precedes cell excitation. Supported in part by a grant from the American Diabetes Association.

Th-AM-H7

HYDROLYSIS RESISTANT GTP ANALOGUES STIMULATE EXOCYTOSIS IN BOVINE ADRENAL CHROMAFFIN CELLS. ((I.M. Robinson, A.F. Oberhauser, K. Okano, and J.M. Fernandez.)) Dept. of Physiology and Biophysics, Mayo Clinic, Rochester, MN 55905.

We have used the whole-cell patch clamp technique to measure secretion in adrenal chromaffin cells. Using the patch pipette to perfuse the cell, it was possible to stimulate an exocytotic response with the non-hydrolysable GTP analogue, GppNHp. When cells were stimulated by GppNHp in the presence of 30 nM $[Ca^{2+}]_i$, only 6 of 9 cells responded. In contrast, 100% of cells responded when stimulated in the presence of 200 nM $[Ca^{2+}]_i$. Perfusion of the cells with either 30nM or 200 nM Ca^{2+}-buffered solutions did not stimulate a secretory response in the absence of guanine nucleotides. The response to GppNHp could be inhibited by either GDPβS or by GTP. This suggests that a sustained activation of a GTP-binding protein is sufficient to cause exocytotic fusion. This response was also observed when the cells were stimulated in a nominally Ca^{2+} free extracellular solution, suggesting that the response was independent of Ca^{2+} entry into the cell. Use of the caged form of GTPγS has shown that the cells still secrete in response to GTP analogues after 20 minutes in the whole-cell configuration, a time in which cytosolic factors of molecular weights smaller than 110 kDa would have leaked out of the cell. The use of this technique enabled the recording of individual step increases in cell membrane capacitance of 2-3fF. These steps are presumably due to the incorporation of individual secretory vesicles into the plasma membrane. When amperometry was used concomitantly with capacitance measurements to study the release of catecholamines from the cells, many "step"-increases in capacitance were accompanied by simultaneous spikes in the amperometric recordings. The maximum rate of capacitance change induced by GTPγS was accompanied by the highest frequency of amperometric spikes. These two results argue against the possibility that the guanine nucleotide analogues are merely exerting their effect on cell membrane capacitance by inhibiting endocytosis.These results suggest that a GTP-binding protein can stimulate exocytosis, is not free to diffuse and as such could be one of the components of an hypothesised fusion pore scaffold.

Th-AM-H8

ASSOCIATION OF ENDOGENOUS Go-ALPHA SUBUNIT WITH THE PURIFIED N-TYPE VOLTAGE-DEPENDENT CALCIUM CHANNEL. ((M.W. McEnery*, A.M. Snowman#, and S.H. Snyder#)) *Dept. of Physiol. and Biophysics, Case Western Reserve Univ. Sch. of Med., Cleveland, OH 44106 and #Dept. of Neuroscience, The Johns Hopkins Univ. Sch. of Med., Baltimore, MD 21205.

Modulation of the omega-conotoxin GVIA (CTX) sensitive N-type voltage-dependent calcium channel (VDCC) by numerous neurotransmitters and guanine nucleotides suggests a dynamic interaction between activated G-protein alpha subunits and the N-type VDCC. Our previous report on the purification of the N-type VDCC based upon its ability to bind [^{125}I]CTX with picomolar affinity (McEnery, et al., (1991) Proc. Natl. Acad. Sci. (USA) **88**, 11095; McEnery (1993) Methods in Pharmacol. **7**: 3) and the observation of Gs-alpha associating with L-type VDCC (Hamilton, et al., (1991) J. Biol. Chem. **261**: 19528), suggested a possible association of N-type VDCC with an endogenous G-alpha subunit. The addition of the G-protein activator AlF_4- modulated the [^{125}I]CTX binding characteristics of the solubilized N-type VDCC. Further immunological analyses employing G-alpha subunit-specific antibodies to monitor the cofractionation of G-alpha with [^{125}I]CTX binding activity throughout the purification procedure indicate the selective recovery of Go-alpha in the purified N-type VDCC preparation, as neither Gs-alpha, Gi-alpha nor G-beta/gamma could be detected. Furthermore, Go-alpha associated with N-type VDCC acted as a substrate for pertussis toxin-dependent ADP-ribosylation only upon the addition of exogenous G-beta/gamma subunits. These results strongly suggest a high affinity complex between an activated Go-alpha and N-type VDCC maintained throughout biochemical purification of the N-type VDCC.

Th-AM-H9

REGULATION OF THE EXOCYTOTIC FUSION SCAFFOLD BY GTP AND Ca^{2+} BINDING PROTEINS. ((A.F. Oberhauser, I.M. Robinson, V. Balan and J.M. Fernandez)) Dept. of Physiology and Biophysics, Mayo Clinic, Rochester MN 55905.

We have recently proposed that the formation of the exocytotic fusion pore is directed by a macromolecular protein scaffold. We suggested that Ca^{2+} and GTP-binding proteins of the rab3 family are some of the components of the scaffold. We investigated the interaction between the Ca^{2+} and GTP binding proteins by perfusing patch-clamped mast cells with caged Ca^{2+} compounds and guanine nucleotides and found that a rapid burst of exocytotic fusion can be induced by flash photolysis of DM-nitrophen (10 mM plus 3 mM Ca^{2+}) in the presence of 1.5 mM GTP. Each burst is composed of 30-50 fusion events (measured as stepwise increases in cell membrane capacitance). Exocytotic fusion stopped a few seconds after the UV exposure, reflecting the return of $[Ca^{2+}]_i$ to resting levels (measured with 100 μM fura-2) as the uncaged Ca^{2+} diffused out of the cell and was replaced with fresh caged Ca^{2+}. In experiments in which GTP was omitted from the pipette solution, no fusion events were observed. Similar to the effect of GTPγS, the secretory response induced by Ca^{2+} does not washout: flash photolysis of caged Ca^{2+}, after as long as 25 min of cell perfusion, is still able to induce complete degranulation, indicating that the target Ca^{2+} binding protein is closely associated with the scaffold regulating exocytosis. We also studied the role of other types of proteins in exocytosis by perfusing mast cells with synthetic peptides that have been shown to inhibit exocytosis in other cell types. Peptides for the C2 domain of synaptotagmin (1 mM) and for the most conserved region of the annexins (0.5 mM) did not inhibit the exocytotic response elicited by GTPγS or the combination of Ca^{2+} and GTP, even after delaying the stimulus by more than 20 min. A peptide based on the N-terminus of hARF1 (2-17; 25 μM) blocked the exocytotic response triggered by a mixture of Ca^{2+} (800 nM) and GTP (1 mM). This peptide also inhibited the secretory response elicited by flash photolysis of caged Ca^{2+} (with 1 mM GTP) or caged GTPγS. These results implicate ARF or a target protein of ARF as a component of the exocytotic fusion pore scaffold.

MECHANOENZYMES

Th-PM-Sym-1

ACTIN POLYMERIZATION AND THE PROPULSION OF *LISTERIA MONOCYTOGENES* ((J. A. Theriot)) Whitehead Institute, Cambridge, MA 02142.

Listeria monocytogenes, a Gram-positive bacterium, is a facultative intracellular parasite that grows directly in the cytoplasm of host cells and uses a form of actin-based motility for intra- and intercellular spread. Moving intracellular *L. monocytogenes* are associated with a polarized "comet tail" made up of short crosslinked actin filaments. Fluorescence photoactivation of labeled actin filaments in the tail indicates that the actin filaments remain stationary in the cytoplasm as the bacterium moves. The bacterium induces assembly of actin filaments near its surface, which are then released and crosslinked into the stationary tail structure. The bacterial surface protein ActA is required for actin assembly. In infected cells, the host actin monomer-binding protein profilin is localized to the surface of motile *L. monocytogenes*, and profilin binding is correlated with rapid and efficient movement. This localization depends on a proline-rich domain of ActA. A distinct domain of ActA appears to be involved in actin filament nucleation. Actin-based *L. monocytogenes* motility can be faithfully reconstituted in cytoplasmic extracts of *Xenopus laevis* eggs. Extracts from which profilin has been depleted do not support bacterial motility. There is no evidence for the involvement of myosin in the propulsion of *L. monocytogenes*. Actin polymerization itself may produce propulsive force through a "Brownian ratchet" mechanism.

Th-PM-Sym-2

KINESIN CAN SUPPORT MINUS-END DIRECTED, DEPOLYMERIZATION-DRIVEN MOTILITY BY COUPLING OBJECTS TO SHORTENING MICROTUBULES. ((J.R. McIntosh, V.A. Lombillo, C. Nislow, V.I. Gelfand*, T.J. Yen#, and R.J. Stewart&)) Dept. of Molecular, Cellular, and Developmental Biology, Univ. Colorado, Boulder, 80309; * Univ. Illinois, Urbana, 61801; # Fox Chase Cancer Center, Philadelphia, PA 19111; & Rowland Inst. Cambridge, MA 02142.

Chromosomes and vesicles will bind to microtubules (MTs) growing from detergent-extracted pellicles of Tetrahymena and move in (toward the minus MT end) when the MTs depolymerize, even without ATP (Coue et al., 1991. JCB 112:1165). We have investigated this motility with antibodies (Abs) to known kinetochore proteins. Function blocking Abs to cytoplasmic dynein have no effect, but motility is stopped by Abs to the heavy chain of kinesin that bind a broad range of kinesin-like proteins (KLPs) (Rodionov et al., 1991. PNAS 88: 4956). Chromosome speed is slowed >3-fold by Abs against the kinetochore KLP, CENP-E (Yen et al., Nature 359: 536). Abs to other kinetochore antigens had no effect. Depolymerization-driven motility has been recon-stituted using latex micro-spheres, coated with HeLa kinesin. Without ATP, these move in at 23 ± 6 um/min (N=26), about the speed of chromosomes in our assay. With ATP and tubulin they move out at ca. 50 um/min. With ATP but w/o tubulin, they come in with the MT ends at ca. 50 um/min. Beads coated with a nonmotile chimeric KLP move with MT disassembly at 186 ± 84 um/min (N=45). Our data suggest that KLPs can bind MTs in the absence of ATP by associations that permit motility driven by the free energy released with tubulin depolymerization.